

# Evaluation of the mechanism of luminescence and structure-efficiency relations of vanadate phosphors

Zom, Jeffrey; van der Kolk, Erik

DOI

10.1016/j.jlumin.2025.121397

**Publication date** 

**Document Version** Final published version

Published in Journal of Luminescence

Citation (APA)

Zom, J., & van der Kolk, E. (2025). Evaluation of the mechanism of luminescence and structure-efficiency relations of vanadate phosphors. *Journal of Luminescence*, *286*, Article 121397. https://doi.org/10.1016/j.jlumin.2025.121397

Important note

To cite this publication, please use the final published version (if applicable). Please check the document version above.

Copyright

Other than for strictly personal use, it is not permitted to download, forward or distribute the text or part of it, without the consent of the author(s) and/or copyright holder(s), unless the work is under an open content license such as Creative Commons.

Please contact us and provide details if you believe this document breaches copyrights. We will remove access to the work immediately and investigate your claim.



Contents lists available at ScienceDirect

# Journal of Luminescence

journal homepage: www.elsevier.com/locate/jlumin



Full Length Article

# Evaluation of the mechanism of luminescence and structure-efficiency relations of vanadate phosphors

Jeffrey Zom <sup>[D]</sup>,\*, Erik van der Kolk

Luminescence Materials, Delft University of Technology, Mekelweg 15, 2629 JB, Delft, the Netherlands

### ARTICLE INFO

## Keywords: Vanadate Luminescence Charge transfer Polaron Self-trapped exciton

# ABSTRACT

Over the past decades, research on novel vanadate phosphors has gained increasing attention. The widely accepted mechanism that explains their broad absorption in the ultraviolet and their broad luminescence in the visible spectrum is based on energy levels derived from the molecular orbitals of isolated  $VO_4$  tetrahedra, in which the excitation is described as a charge transfer excitation. In this work, we critically examine both this mechanism of luminescence in vanadates and two mechanisms that are often used to explain their luminescent efficiency. By correlating published optical properties (e.g. excitation energies, Stokes shifts, and emission bandwidths) with structural properties (e.g. bond lengths and bond angles) on 77 different vanadate phosphors, we find that there is no strong evidence in favour of the proposed mechanisms used to describe luminescence as well as quenching thereof. Instead, we suggest a mechanism in which the luminescent charge transfer state is not directly formed upon photoexcitation but rather formed after initial electron trapping following bandgap excitation. The resulting luminescent state is, therefore, likely to be more appropriately termed a self-trapped exciton.

## 1. Introduction

From the 1970s, George Blasse pioneered the research field of phosphors based on closed-shell transition metal ions. One such ion of significant interest is V<sup>5+</sup>, which in oxide structures almost exclusively forms VO<sub>4</sub> tetrahedra that ought to be responsible for both broadband absorption of ultraviolet light and the emission of broadband visible light. At that time, research was mainly focused on gaining fundamental knowledge: the mechanism of luminescence and the structure-property relations [1]. Despite theoretical advancements, shortly before he retired at the end of the twentieth century, Blasse noted that, based on the latest EPR studies from the research group of Van der Waals, a detailed mechanism of luminescence in vanadates remained unknown: 'The excited state cannot even approximately be described in terms of molecular orbitals of the tetrahedral ion.' [2,3]. Nevertheless, this mechanism of luminescence in vanadates kept on being used and research shifted focus ever since from deepening theoretical knowledge to exploration of a large number of novel compositions for practical applications.

As a notable exception that has gained a lot of attention in the field, Nakajima et al. published a paper in 2010 in which they proposed to have found a novel relationship between structural properties and internal quantum efficiency (IQE) in vanadates [4]. They proposed two

criteria to obtain a high IQE: a small separation between vanadium atoms and a large separation between vanadium and other cations. This is different from the hypothesis made earlier by Blasse in 1977 [5]. He suggested that a high rigidity of the  $\rm VO_4$  tetrahedron is required for a high IQE, namely those with structures in which ions with a small polarisability lie in the extension of the V-O bonds. It is Nakajima's proposed structure-property relationship that has been cited often in the last decade to explain differences in IQE between different compounds.

In order to efficiently explore the immense space of possible vanadate compositions to find novel and highly efficient phosphors, theoretical knowledge on the mechanisms of both luminescence and quenching is paramount. However, these mechanisms for this class of phosphors have not been a strong topic of debate in the last few decades. Therefore, the main focus of this study is to discuss the current mechanisms proposed for luminescence and quenching thereof in vanadate phosphors.

In aid of this, we have collected a large amount of data on the luminescent and structural properties of 77 vanadate compositions from the literature. This data allows us to test the proposed optical and structural correlations mentioned earlier. The discussion will be done in two parts. Firstly, we discuss how the data can provide new insights into the mechanism of luminescence and how they stand in contrast to the widely accepted mechanism. Secondly, we show that the data do not

E-mail address: j.zom@tudelft.nl (J. Zom).

<sup>\*</sup> Corresponding author.

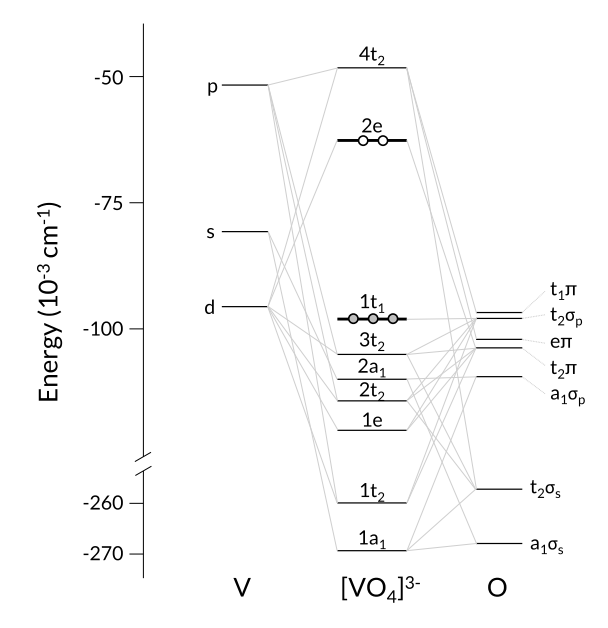


**Fig. 1.** Molecular orbital diagram of the tetrahedral vanadate ion  $[VO_4]^{3-}$ . The molecular orbital with symmetry label  $1t_1$  is the highest occupied molecular orbital, whereas that with 2e is the lowest unoccupied molecular orbital. Reproduced from Fotiev et al. [7].

support the structure-efficiency relations put forth by both Blasse and Nakajima. Before starting our discussion, we provide a brief description of the mechanism of luminescence in vanadates that has been widely accepted. This mechanism was first proposed in 1958 by Ballhausen and Liehr on the basis of the Van Vleck molecular orbital theory [6].

Based on molecular orbital (MO) theory, the origin of luminescence from closed shell configuration transition metal ions coordinated by four oxygen atoms (transition metals with no d-electrons, also described as d0-tetroxo-ions), is thought to be the result of the transition of an electron between a triply-degenerate non-bonding  $t_1$  MO to a doubly degenerate anti-bonding  $e^*$  MO, which are respectively the highest occupied and lowest unoccupied MOs [1,7]. Fig. 1 shows the molecular orbitals of the [VO<sub>4</sub>]<sup>3-</sup> centre formed by the combination of atomic orbitals from vanadium and oxygen [7]. As  $t_1$  is only formed by linear combinations of oxygen  $2p_{\pi}$  orbitals, and  $e^*$  is mainly characterised by 3d orbitals of vanadium [3,7], the transition is often described as a charge transfer (CT) transition in which the oxygen atoms collectively transfer electron density to their central vanadium ion. In  $T_d$  symmetry, the ground state with electron configuration  $t_1^6$  is represented by the Mulliken symbol  ${}^{1}A_{1}$ , while the excited-state configuration  $t_{1}^{5}2e$  gives rise to the excited states of symmetry, in order of increasing energy, the triplet states  ${}^3T_1$  and  ${}^3T_2$ , and the singlet states  ${}^1T_1$  and  ${}^1T_2$ . Fig. 2 shows an energy level diagram of the processes that occur between these states. The energy difference between the singlet states was calculated to be on the order of 1 eV, while it is only a few tens of meV between the triplet states [5]. Only the transition between <sup>1</sup>A<sub>1</sub> and <sup>1</sup>T<sub>2</sub> is both spin and electric-dipole allowed, whereas  ${}^{1}A_{1} \rightarrow {}^{1}T_{1}$  is electric-dipole forbidden,  ${}^{1}A_{1} \rightarrow {}^{3}T_{2}$  is spin forbidden, and  ${}^{1}A_{1} \rightarrow {}^{3}T_{1}$  is both electric-dipole and spin forbidden. The excitations are then described as transitions from the ground state to the singlet states, whereas luminescence occurs, after intersystem crossing, from the triplet states to the ground state. The broad character of the excitation and emission spectra is explained by significant lattice relaxations that accompany the transitions. The long excited-state lifetime that is often measured, on the order of microseconds, can then be explained by the forbidden character of the  ${}^3T_2/{}^3T_1$  $\rightarrow$  <sup>1</sup>A<sub>1</sub> transitions. Within this theory, both excitation and emission processes are described as transitions involving the whole [VO<sub>4</sub>]<sup>3-</sup> centre and the four oxygens never lose their equivalence.

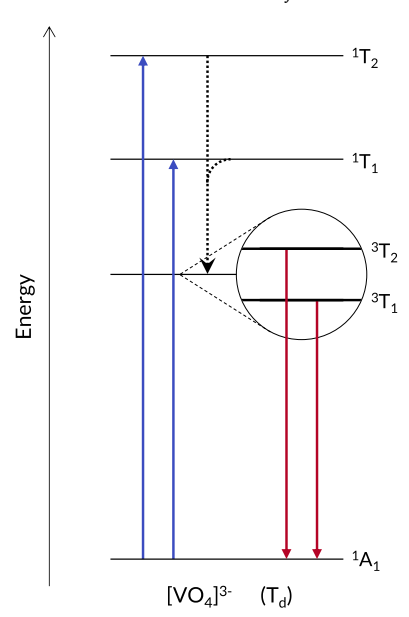


**Fig. 2.** Energy level diagram illustrating electronic transitions in the tetrahedral vanadate ion  $[VO_4]^{3-}$  ( $T_a$  symmetry). Blue arrows indicate transitions accompanying absorption from the ground state  $(^1A_1)$  to the excited singlet states  $(^1T_1, ^1T_2)$ . Red arrows indicate transitions accompanying emission from the triplet excited states  $(^3T_1, ^3T_2)$  back to the ground state. The inset highlights the small energetic difference between the triplet states.

## 2. Methods

Publications reporting the luminescent and structural properties of vanadate phosphors were gathered using the search engines Scopus and Google Scholar. Only data in which measurements were performed at room temperature were used. Furthermore, compounds in which the host lattices contained optically active ions (e.g. the commonly reported Bi<sup>3+</sup> and Eu<sup>3+</sup> containing vanadates) or (partly) contained anions other than oxygen (e.g. Sr<sub>2</sub>VO<sub>4</sub>Cl) were excluded. Due to the small ionic radius of V<sup>5+</sup>, its coordination number is rarely greater than 4, with only a few known exception cases with coordination number 5 (e.g.  $V_2O_5$ ,  $Ca_2V_2O_7$ ,  $MV_3O_8$  (M=K,Rb,Cs) [8–10]) and 6 (e.g.  $Ba_2MVO_6$ , M = Bi, La, Y, Ln [11,12]). As the coordination number of  $V^{5+}$  is expected to strongly influence optical properties, and because of the lack of data on vanadates with higher coordination numbers, only compounds with tetrahedral coordinated vanadium atoms were included. Of the resulting 119 publications [4,7,13–129], the following properties were noted to the extent that they were available: Internal quantum efficiency, highest wavelength of the local maxima of the excitation spectrum, wavelength of the maximum, and full width half maximum, of the emission spectrum, average excited-state lifetime, space group of the crystal structure, and structural arrangement type of the [VO<sub>4</sub>]<sup>3-</sup> centres (isolated (ortho-), dimer (pyro-), chain (meta-), etc.). The highest quality Powder Diffraction Files (PDFs) matching the composition and space group were obtained from the ICDD database as Crystallographic Information Files (CIFs). Through this approach, we obtained the optical properties of 77 different vanadate phosphors, including the crystalline characteristics of 55 of them (a valid CIF was not available for some compounds). Custom Python programmes were written to read out the CIFs and analyse the structure-property relations. Linear regression between tested parameters was performed using an ordinary least squares model implemented in the Python package statsmodels. The quality of the fit was evaluated using the coefficient of determination  $(R^2)$  and the p-value associated with the slope parameter. Relationships with p < 0.01 were considered statistically significant. Table 1 gives a list of selected properties of all vanadates investigated in this study.

Table 1
Spectroscopic and structural properties of all studied vanadates (reported for room temperature). The quantum yield and excited-state lifetime are the highest reported values, whereas the 1<sup>st</sup> excitation maximum, emission maximum and emission width are average values along with their standard deviation. \*The lifetimes reported in these publications appear to have been calculated incorrectly.

		Yield (%)	Maximum (eV)	Maximum (eV)	Width (eV)	lifetime (μs)	Diffraction File	Type	
	$AgCa_2Zn_2V_3O_{12}$	-	3.71	2.18	0.62	158	00-050-0393	isolated	[13]
	$Ba_2V_2O_7$	47.5	$3.60 \pm 0.09$	$2.44 \pm 0.04$	$0.65 \pm 0.050$	1.39	00-039-1432	dimer	[7,14–19],
	$Ba_3MgV_4O_{14}$	-	3.78	2.47	-	-	04-022-4896	dimer	[20]
	Ba <sub>3</sub> V <sub>2</sub> O <sub>8</sub>	7.3	$3.61 \pm 0.02$	$2.50 \pm 0.05$	$0.62 \pm 0.024$	16.9	00-029-0211	isolated	[7,21–24]
	Ba <sub>3</sub> YV <sub>2</sub> O <sub>8</sub>	-	$3.74 \pm 0.13$	$2.67 \pm 0.15$	$0.62 \pm 0.005$	-	-	isolated	[22,25]
	$Ba_3ZnV_4O_{14}$	-	3.75	2.40	-	-	04-022-4897	dimer	[20]
	Ba <sub>9</sub> LaV <sub>7</sub> O <sub>24</sub>	_	3.54	2.44	0.54	-	-	isolated	[26]
	Ca <sub>3</sub> V <sub>2</sub> O <sub>8</sub>	0.7	3.85	$2.30 \pm 0.07$	0.82	_	04-011-1043	dimer	[4,7]
	Ca <sub>4</sub> LaV <sub>3</sub> O <sub>13</sub>	31.5	3.49	2.34	0.54	1.89	04-027-0897	isolated	[27]
)	Ca <sub>5</sub> Mg <sub>3</sub> ZnV <sub>6</sub> O <sub>24</sub>	58	3.58	2.43	0.57	-	04-009-9724	isolated	[28]
1		41.6	$3.55 \pm 0.08$	$2.32 \pm 0.02$	$0.61 \pm 0.054$	11.01	00-034-0014	isolated	[29–32]
	Ca <sub>5</sub> Mg <sub>4</sub> V <sub>6</sub> O <sub>24</sub>	21.9		$2.32 \pm 0.02$ $2.28 \pm 0.02$					
2	Ca <sub>5</sub> Zn <sub>4</sub> V <sub>6</sub> O <sub>24</sub>		$3.45 \pm 0.04$		$0.54 \pm 0.049$	7.34	00-053-1164	isolated	[29,32,33]
3	Ca <sub>9</sub> LaV <sub>7</sub> O <sub>24</sub>	-	3.54	2.53	0.55	-	-	isolated	[26]
4	Cs <sub>2</sub> CaV <sub>2</sub> O <sub>7</sub>	-	3.41	$2.21 \pm 0.01$	$0.65 \pm 0.050$	46	04-017-2249	dimer	[34,35]
5	$Cs_2ZnV_4O_{12}$	-	3.77	2.30	0.61	-	-	chain	[36]
5	Cs <sub>3</sub> VO <sub>4</sub>	90	3.32	2.40	0.69	-	-	-	[37]
7	$Cs_5V_3O_{10}$	85.2	$3.34 \pm 0.03$	2.39	$0.65 \pm 0.056$	0.0245	-	-	[38–40]
3	CsBaVO <sub>4</sub>	-	-	2.52	-	17	-	isolated	[7]
9	CsCaVO <sub>4</sub>	-	-	2.55	-	20	-	isolated	[7]
)	CsSrVO <sub>4</sub>	-	-	2.53	-	20	-	isolated	[7]
1	CsVO <sub>3</sub>	95.8	$3.37 \pm 0.08$	$2.35 \pm 0.04$	$0.62 \pm 0.079$	16.9	04-010-2780	chain	[7,37,41–46]
2	InVO <sub>4</sub>	-	$3.89 \pm 0.08$	$2.21\pm0.10$	$0.60 \pm 0.068$	69	00-048-0898	isolated	[47–51]
3	K <sub>2</sub> CaV <sub>2</sub> O <sub>7</sub>	-	3.53	2.30	0.64	-	04-020-0187	dimer	[35]
4	K <sub>2</sub> CsYV <sub>2</sub> O <sub>8</sub>	-	3.38	2.46	0.63	-	04-001-9719	isolated	[52]
5	$K_2MgV_2O_7$	-	3.52	$2.33 \pm 0.02$	$0.61 \pm 0.020$	22	04-009-0692	dimer	[35,53]
5	$K_2ZnV_2O_7$	-	-	2.46	0.70	53	04-023-1110	dimer	[53]
7	K <sub>3</sub> LaV <sub>2</sub> O <sub>8</sub>	26	3.46	2.39	0.60	12.88	00-051-0094	isolated	[54]
3	K <sub>3</sub> YV <sub>2</sub> O <sub>8</sub>	47	3.67	2.39	0.59	18.12	04-019-7228	isolated	[54]
		-	-	2.49	0.39	17	04-019-7228	isolated	[7]
9	KBaVO <sub>4</sub>				0.64 + 0.070				
	KCa <sub>2</sub> Mg <sub>2</sub> V <sub>3</sub> O <sub>12</sub>	78.9	$3.67 \pm 0.22$	$2.34 \pm 0.06$	$0.64 \pm 0.070$	5.72	00-024-1044	isolated	[55–59]
l	$KCa_2Zn_2V_3O_{12}$	19.2	$3.41 \pm 0.22$	$2.38 \pm 0.03$	$0.62 \pm 0.025$	6.9	04-027-6626	isolated	[60,61]
2	KCaVO <sub>4</sub>	-	-	2.52	-	8	00-056-0125	isolated	[7]
3	$KLa_5V_2O_{13}$	-	3.68	2.67	0.16	-	-	isolated	[62]
4	KSrVO <sub>4</sub>	-	3.50	$2.42 \pm 0.09$	0.76	7	04-027-7976	isolated	[7,63]
5	KVO <sub>3</sub>	4	$3.26 \pm 0.18$	$2.26 \pm 0.01$	0.73	-	04-008-9439	chain	[7,41,45]
5	LaVO <sub>4</sub>	-	3.94	2.09	0.60	-	04-008-8070	isolated	[64]
7	LiBaVO <sub>4</sub>	-	-	2.55	-	6	-	isolated	[7]
3	$LiCa_2Mg_2V_3O_{12}$	42.5	$3.59 \pm 0.11$	$2.42 \pm 0.02$	$0.57 \pm 0.009$	73	04-015-3927	isolated	[57,65,66]
9	LiCa <sub>2</sub> MgSrV <sub>3</sub> O <sub>12</sub>	32.5	3.59	2.50	0.62	4.8	-	isolated	[67]
)	LiCa <sub>3</sub> MgV <sub>3</sub> O <sub>12</sub>	69.3	$3.80 \pm 0.07$	$2.55 \pm 0.06$	$0.70 \pm 0.066$	17.52	01-086-5533	isolated	[68–74]
1	LiCa <sub>3</sub> ZnV <sub>3</sub> O <sub>12</sub>	40.1	$3.70 \pm 0.09$	$2.52 \pm 0.03$	$0.67 \pm 0.056$	12.4	01-086-5532	isolated	[74-81]
2	LiCaVO <sub>4</sub>	-	-	2.54	-	4	-	isolated	[7]
3	LiSrVO <sub>4</sub>	_	3.72	$2.42 \pm 0.04$	0.60	6.86	_	isolated	[7,82]
4	LiZnVO <sub>4</sub>	_	$3.67 \pm 0.24$	$2.35 \pm 0.04$	$0.56 \pm 0.048$	105	04-016-8375	chain	[83–85]
5	LuVO <sub>4</sub>	_	$4.17 \pm 0.06$	$2.77 \pm 0.08$	$0.54 \pm 0.205$	17	00-017-0880	isolated	[86–88]
5	Mg <sub>2</sub> BaV <sub>2</sub> O <sub>8</sub>		3.90	2.31	0.69	1463*	01-072-2159	isolated	[89]
7	$Mg_2V_2O_7$	-	-	2.30	-	-	04-008-6711	dimer	[7]
, 3		15.8	$3.73 \pm 0.12$	$2.19 \pm 0.14$	$0.58 \pm 0.087$	- 950*	01-073-0207	isolated	[7,14,23,90]
	Mg <sub>3</sub> V <sub>2</sub> O <sub>8</sub>								
9	Na <sub>2</sub> Mg <sub>2</sub> YV <sub>3</sub> O <sub>12</sub>	22.4	$3.61 \pm 0.13$	$2.38 \pm 0.05$	$0.60 \pm 0.059$	6.1	00-049-0412	isolated	[56,91–95]
)	NaBaVO <sub>4</sub>	-	-	2.53	-	6	04-008-3759	isolated	[7]
1	NaCa <sub>2</sub> Mg <sub>2</sub> V <sub>3</sub> O <sub>12</sub>	36	$3.73 \pm 0.06$	$2.47 \pm 0.06$	$0.69 \pm 0.063$	5.9	04-015-3927	isolated	[57,59,96–99]
2	NaCa <sub>2</sub> Zn <sub>2</sub> V <sub>3</sub> O <sub>12</sub>	11.4	3.6	2.52	0.58	9550*	04-014-2972	isolated	[100]
3	NaCaVO <sub>4</sub>	-	-	2.51	-	3	04-009-4198	isolated	[7]
4	$\mathrm{NaMg}_2\mathrm{V}_3\mathrm{O}_{10}$	26	3.33	2.39	0.69	-	04-015-9247	trimer	[101]
5	$NaMg_4V_3O_{12}$	61	3.48	2.34	0.66	1.77	04-013-3807	isolated	[102]
5	$\mathrm{NaSr}_{2}\mathrm{Mg}_{2}\mathrm{V}_{3}\mathrm{O}_{12}$	87.3	3.85	$2.49 \pm 0.04$	$0.68 \pm 0.025$	6.15	04-008-4894	isolated	[56,59]
7	NaSrVO <sub>4</sub>	-	-	2.50	-	4	04-008-3758	isolated	[7]
3	NaVO <sub>3</sub>	-	-	$2.11\pm0.01$	-	-	04-013-7268	chain	[7,41]
9	Rb <sub>2</sub> CaV <sub>2</sub> O <sub>7</sub>	-	$3.65 \pm 0.04$	$2.23 \pm 0.03$	$0.66 \pm 0.055$	46	00-056-0367	dimer	[34,35]
)	$Rb_2ZnV_4O_{12}$	-	3.82	2.02	0.47	-	-	chain	[36]
l	Rb <sub>3</sub> LuV <sub>2</sub> O <sub>8</sub>	85	3.43	2.48	0.56	23.75	00-056-1429	isolated	[103]
2	Rb <sub>3</sub> YV <sub>2</sub> O <sub>8</sub>	71	3.41	2.48	0.54	20.06	04-027-5719	isolated	[103]
3	Rb <sub>5</sub> V <sub>3</sub> O <sub>10</sub>	-	3.44	2.42	0.59	-	-	-	[40]
4	RbBaVO <sub>4</sub>	-	-	2.52	-	21	00-055-0516	isolated	[7]
							00-033-0310	isoiateu	
5	RbCaLaV <sub>2</sub> O <sub>8</sub>	10	3.43	-	-	-	-	- incl-+ 1	[104]
5	RbCaVO <sub>4</sub>	-	-	2.52	-	16	-	isolated	[7]
7	RbSrVO <sub>4</sub>	-	-	2.52	-	25	-	isolated	[7]
3	RbVO <sub>3</sub>	79	$3.40 \pm 0.12$	$2.34 \pm 0.04$	$0.65 \pm 0.105$	-	04-008-9440	chain	[7,41,45,105,1
	0.110	FF 1	2.75 . 0.02	2 54 + 0 00	$0.72 \pm 0.000$	8.5	01-079-7028	isolated	[50,107-109]
<b>∂</b> )	ScVO <sub>4</sub> Sr <sub>2</sub> V <sub>2</sub> O <sub>7</sub>	55.1 14	$3.75 \pm 0.02$	$2.54 \pm 0.08$ $2.31 \pm 0.07$	$0.72 \pm 0.008$ 0.71	6.5	04-011-5542	dimer	[7,14,15]

3

Table 1 (continued)

Index	Compound	Quantum Yield (%)	Excitation Maximum (eV)	Emission Maximum (eV)	Emission Width (eV)	Excited-state lifetime (μs)	Powder Diffraction File	[VO <sub>4</sub> ] <sup>3-</sup> Type	Reference(s)
71	Sr <sub>3</sub> LaV <sub>3</sub> O <sub>12</sub>	32.7	3.53	2.39	0.62	4.24	-	-	[110]
72	$Sr_3V_2O_8$	82	$3.61 \pm 0.04$	$2.36 \pm 0.05$	$0.63 \pm 0.074$	29.2	01-079-5615	isolated	[4,7,23,111,112]
73	$Sr_6V_2O_{11}$	40	3.31	2.28	0.48	3.130	-	-	[113]
74	$Sr_9LaV_7O_{24}$	-	3.54	2.44	0.54	-	-	-	[26]
75	$YVO_4$	-	$3.90 \pm 0.09$	$2.76 \pm 0.12$	$0.67 \pm 0.097$	38	00-017-0341	isolated	[88,114-119]
76	$Zn_2V_2O_7$	-	$3.71 \pm 0.06$	$2.34 \pm 0.01$	$0.45 \pm 0.025$	-	01-070-9441	dimer	[120,121]
77	$Zn_3V_2O_8$	60	$3.51 \pm 0.06$	$2.22\pm0.07$	$0.62 \pm 0.065$	741.3*	04-019-7360	isolated	[14,37,90,122–129]

### 3. Results & discussion

#### 3.1. Discussion on localised excitation

We will start our discussion on the description of the excitation in vanadate phosphors as a (localised) charge-transfer transition within the vanadate group. We will discuss how the excitation spectra differ both in shape and position from what would be expected based on MO-theory, as well as how the energy of excitation and emission appear uncorrelated

### 3.1.1. Shape and extent of excitation spectra

Discrepancies can be found between the shape of the measured excitation spectra and that theoretically predicted. As excitations in vanadates are considered localised transitions, the excitation spectrum is expected to consist of two peaks that belong to the  ${}^{1}A_{1} \rightarrow {}^{1}T_{2}/{}^{1}T_{1}$ transitions. For some reported excitation spectra, they indeed appear to consist of two peaks [18,32,39,54,99]. However, most of the excitation spectra reported are noticeably different, appearing to consist of only one peak [16,47,65,98,113] or more than two [34,40,42,60,104]. More concerning is that the variation in the excitation spectra is also large among different studies on the same compound. For example, for the compound Cs<sub>2</sub>CaV<sub>2</sub>O<sub>7</sub>, one study reports a relatively simple and narrow excitation spectrum, consisting of a relatively narrow band [35], while a different study reports a complex and broad excitation spectrum, consisting of multiple peaks, that continues to have considerable intensity even beyond 10 eV [34]. One study measured similarly complex excitation spectra for all ten vanadates studied [130], demonstrating that efficient high-energy excitation is a general property rather than an exception. These few studies reporting efficient excitation for high energies stand in contrast to the vast majority of the studies, which report a strong drop in the intensity of the excitation spectra towards vacuum UV. This discrepancy can probably be explained by the fact that most studies do not correct (well) for the wavelength-dependent excitation intensity, as commonly used light sources do not have strong emission in the vacuum UV. It could be argued that the very broad excitation spectra that extend into the vacuum UV can be explained by many different localised transitions based on higher-energy MOs within the VO<sub>4</sub> tetrahedra, as suggested by Shul'gin et al. [130]. An alternative explanation for the excitation spectra could be that the excitations correspond to conventional bandgap excitations, whereby their complex and broad shapes are dictated by the optical joint density of states.

# 3.1.2. Onset of excitation spectra

Discrepancies can also be found between the position of onset of the measured excitation spectra and that theoretically predicted. Ronde and Snijder reported a negative linear dependence between the average V-O bond distance and the position of the excitation spectrum [131]. This linear dependence was in agreement with the results of *ab initio* calculations on free  $[VO_4]^{3-}$  ions with different V-O bond distances. Therefore, they hypothesised that excitations in vanadate compounds can indeed be considered as localised transitions in the vanadate group and that the influence of the host lattice on the excitation spectrum would in first order be described by a variation of the average V-O bond distance. However, their experimental data were limited to only 7 compounds, 4

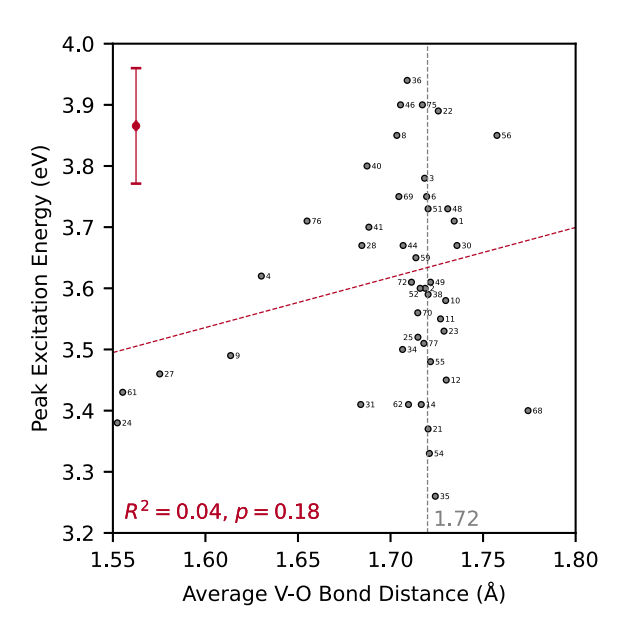


**Fig. 3.** Energy of the  $1^{st}$  local maximum in the excitation spectrum against the mean distance between oxygen and vanadium in the vanadate group. The red line in the top left show the average uncertainty in the energy. The dashed line shows a linear fit with  $R^2 = 0.04$ , p = 0.18, indicating no statistically significant correlation. The numbers adjacent to the datapoints refer to compounds with the same index in Table 1.

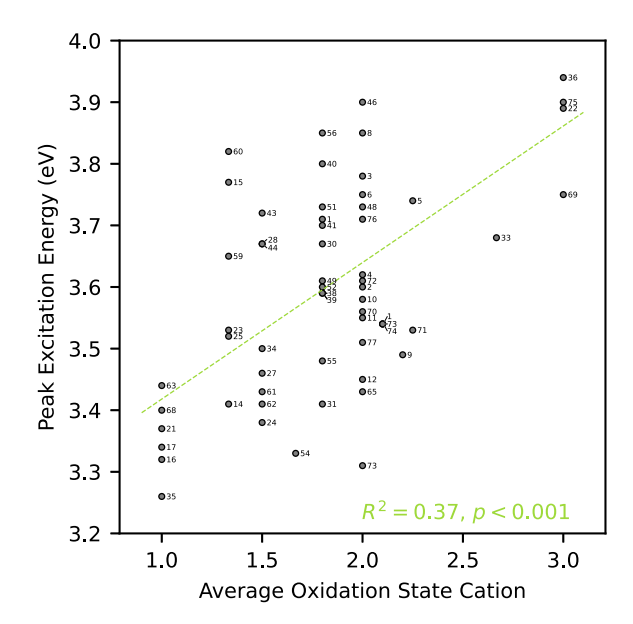
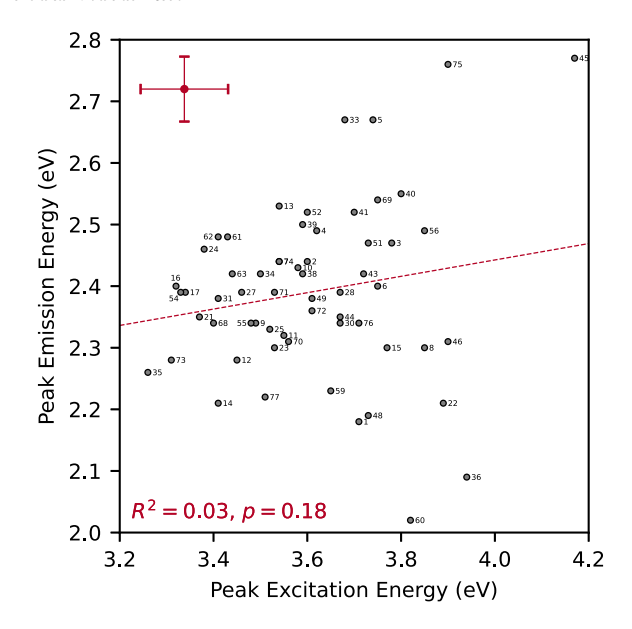


Fig. 4. Energy of the  $1^{st}$  local maximum in the excitation spectrum against the mean (weighed) oxidation state of the cations, other than vanadium, in the phosphor. The green dashed line shows a linear fit with  $R^2 = 0.37$ , p < 0.001, indicating a statistically significant correlation.



**Fig. 5.** Energy of the maximum in the emission spectrum against the energy of the  $1^{st}$  local maximum in the excitation spectrum. The red cross in the top left shows the average uncertainties in the energy. The red dashed line shows a linear fit with  $R^2 = 0.03$ , p = 0.18, indicating no statistically significant correlation.

of which had the same average V-O bond distance of 1.71 Å, but showed a significant variation in the position of the excitation spectrum.

From our gathered data, we have performed a similar analysis, the results of which paint a different picture. Fig. 3 shows the (lowest) peak excitation energy compared to the average V-O bond distance. Most compounds have an average V-O bond distance of  $\sim 1.72~\textrm{Å}$ , indicated in the figure as a vertical grey line, for which the variation in the peak excitation energy is large. There appears to be no linear dependence between the average V-O bond distance and the peak excitation energy. In contrast, the presence of other cations (other than vanadium) appears to have a large influence on the peak excitation energy. In general, the higher the average oxidation state, the higher the peak excitation energy are those containing monovalent cations, such as NaVO3, KVO3, and CsVO3, while those with the highest peak excitation energy are those containing trivalent cations, such as ScVO4, YVO4, and InVO4.

# 3.1.3. Stoke-shift of emission

For local transitions of the type 4f-5d, as in  $Ce^{3+}$ , 3d-3d, as in  $Cr^{3+}$ , and conventional charge transfer excitations, as in Yb3+ doped compounds with their 2+/3+ charge transfer level below the conduction band, the emission peak wavelength is correlated with the excitation peak wavelength. Given that excitation and luminescence in vanadates are described as transitions localised in the VO<sub>4</sub> centre, it is reasonable to expect the same correlation. In Fig. 5, the energy of the (lowest) peak excitation energy is plotted against the peak emission energy. With few exceptions, all vanadates have the first peak in their excitation spectrum within  $\sim 3.3$  to 4.0 eV and their emission peak within  $\sim 2.2$  to 2.6 eV, showing a notably larger variation in the excitation energy. Surprisingly, there appears to be no significant correlation (p = 0.21) between the peak excitation and the peak emission energy. The absence of a correlation between excitation and emission peaks can also be found in early work, where the V5+ concentration was lowered by doping with P<sup>5+</sup>; the wavelength of the onset of the excitation spectrum changes significantly, while the peak wavelength of the emission spectrum stays roughly constant [132].

Thus, it can be concluded that there is no significant correlation between the energy of the absorbing and emitting states. Therefore, we believe that it is unlikely that both excitation and emission take place

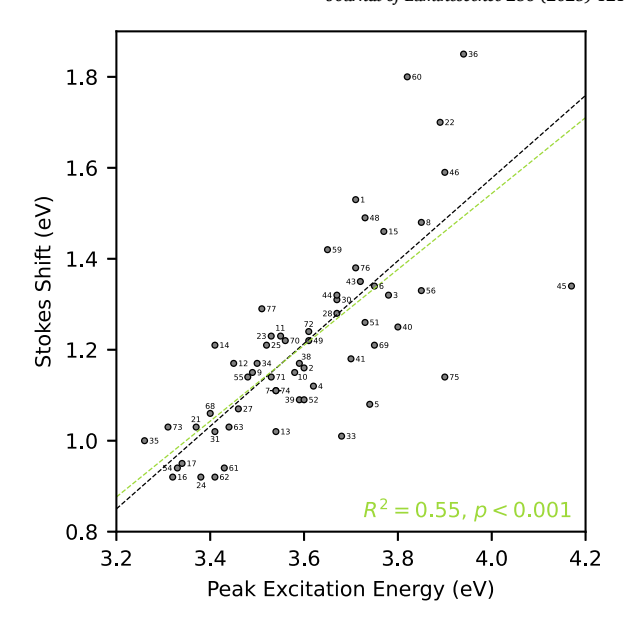


**Fig. 6.** Stokes shift against the energy of the  $1^{st}$  local maximum in the excitation spectrum. The green dashed line shows a linear fit with  $R^2 = 0.55$ , p < 0.001, indicating a statistically significant correlation. For reference, the grey dashed line shows the best fit with a slope of one.

in isolated  $\mathrm{VO}_4$  centres. The absence of a correlation between excitation and emission energy in turn means that there is a correlation between the Stokes shift and excitation energy, as shown in Fig. 6. Note that the term "Stokes shift" is used rather freely for vanadates since the electronic transitions for excitation and emission are not the same (according to the aforementioned mechanism); here it is only defined as the energy difference between the peaks of the excitation and emission spectra, similar to previous research [132].

# 3.2. Proposal of alternative mechanism

Given a clear absence of the two excitation bands in many excitation spectra expected for the  ${}^{1}A_{1} \rightarrow {}^{1}T_{2}/{}^{1}T_{1}$  transitions, the possibility of high energy excitation demonstrated with high-UV excited luminescence, the absence of a clear correlation between the structure of the VO<sub>4</sub> tetrahedra and the excitation peak energy, the strong influence of the composition on the onset of the excitation spectrum, and lastly, the absence of a correlation between the onset of the excitation spectrum and the emission energy, we hypothesize that the excitation process cannot be described as a localised transition within a VO<sub>4</sub> centre, but can be described by typical interband excitation. We further hypothesise that after photoexcitation across the bandgap, the free electron and hole can then localise on a VO<sub>4</sub> centre, effectively forming a self-trapped exciton (STE), which can recombine radiatively. Fig. 7 illustrates the earlier mentioned discrepancy between excitation spectra of Cs<sub>2</sub>CaV<sub>2</sub>O<sub>7</sub>, as well as its emission spectrum, alongside a schematic depicting this luminescent mechanism.

Note that the term self-trapped exciton has occasionally been used previously to describe the excited state in vanadate phosphors [133, 134]. Confusingly, at the same time, these authors continue to describe the excitation process as a localised charge-transfer excitation. The essential difference between these two descriptions lies in the initial state formed after photoexcitation: self-trapped excitons do not form immediately upon excitation. Instead, photoexcitation initially generates free charge carriers or free excitons, which subsequently become self-trapped. This is in contrast to the charge-transfer excitation model, where localisation occurs immediately upon excitation. We will now discuss how this mechanism of bandgap excitation, followed by localised emission, is in line with previous experimental and theoretical research.

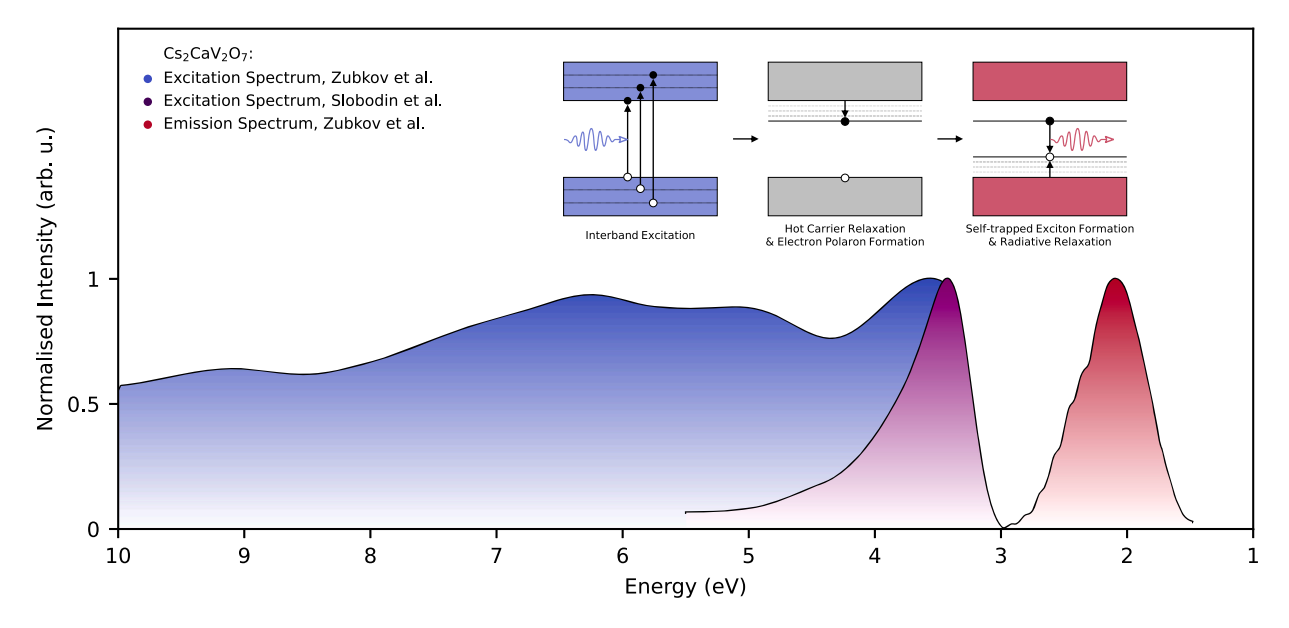


Fig. 7. Normalised excitation spectrum of  $Cs_2CaV_2O_7$  measured at room temperature reported by Zubkov et al. and Slobodin et al. [34,35], respectively coloured blue and purple. The relatively narrow excitation spectrum (coloured purple) represents the often reported excitation spectrum of vanadate phosphors in literature, which is a consequence of inadequate correction for the intensity of the excitation light during measurement. Normalised emission spectrum of  $Cs_2CaV_2O_7$  measured at room temperature reported by Zubkov et al. [34], coloured red. The inset schematic figure illustrates the sequential processes we suggest to be integral to photoluminescence of vanadates: interband excitation, hot carrier relaxation, electron polaron formation, self-trapped exciton formation, and radiative relaxation.

## 3.2.1. Electron polaron formation

Yang. et al. measured the time-dependent formation of  $V^{4+}$  in BiVO<sub>4</sub> after photoexcitation with transient absorption spectroscopy by measuring the formation of the d-d absorbing band [135]. Most importantly, they measured the formation of  $V^{4+}$  to take significantly longer than the instrument response function, suggesting that  $V^{4+}$  is not formed instantaneously when BiVO<sub>4</sub> is photoexcited. They proposed the following mechanism of luminescence in BiVO<sub>4</sub>. First, free electrons and holes would be formed. Then within a picosecond, the electron would localise in  $V^{5+}$  and is described as a small electron polaron, forming  $V^{4+}$ . The hole remains delocalised significantly longer but is eventually also captured, on a nanosecond timescale, by the electron polaron to form a self-trapped exciton. The VO<sub>4</sub> centre on which the STE is located was calculated to be significantly distorted by expansion of the V-O bond lengths.

This mechanism is similar to that described for YVO<sub>4</sub> by Feng et al., in which 3 excited-state configurations of the STE were calculated using density functional theory, in which an electron is localised on V<sup>5+</sup> and the hole is localised on 4, 2 or 1 oxygen atoms [136]. It was calculated that as the number of oxygen atoms accommodating the hole decreases, the energy of the STE decreases, the symmetry of the tetrahedron decreases (from  $D_{2d}$  to  $C_{2v}$  to  $C_s$ ), and the expansion of V-O bond lengths accommodating the hole increases. Note that for the most stable STE configuration, the bond length of V-O accommodating the hole was calculated to increase by  $\sim 0.20\text{Å}$  ( $\sim 12\%$ ). This increase in the length of the V-O bond is similar to that calculated by Blasse (0.15 Å) based on experiments in SiO<sub>2</sub>:V<sup>5+</sup> [5]. The authors then assign the blue emission from YVO<sub>4</sub> to the electron-hole recombination from this STE.

The spontaneous lowering of the symmetry of the vanadate group upon excitation can be expected based on the Jahn-Teller theorem, which states that any nonlinear geometry with a spatially degenerate electronic state will lower its energy by undergoing a geometric distortion that removes that degeneracy [137]. As all excited states of the  $VO_4$  centre with  $T_d$  symmetry described by MO theory are triply degenerate, the centre is expected to undergo a static Jahn-Teller distortion, at which point the group symmetry can no longer be  $T_d$  and the orbital degeneracy of the triplet states must be lifted [3]. Through electro paramagnetic resonance (EPR) studies on the lowest spin triplet state, such a static Jahn-Teller distortion has indeed been shown to occur in

the d0-tetroxo-ions [VO<sub>4</sub>]<sup>3-</sup> [3,138–140] and [CrO<sub>4</sub>]<sup>2-</sup> [139,141]. Photoexcitation was hypothesised to lower the symmetry of the VO<sub>4</sub> centre from  $T_d$  to  $C_{3v}$ , in which the length of a V-O bond is significantly extended, whereas the others remain similar. The observation of excited states with even lower symmetry, such as  $C_s$  in YVO<sub>4</sub>, could then be explained by the reduction of the symmetry of a VO<sub>4</sub> centre that already has a ground state of low symmetry [3].

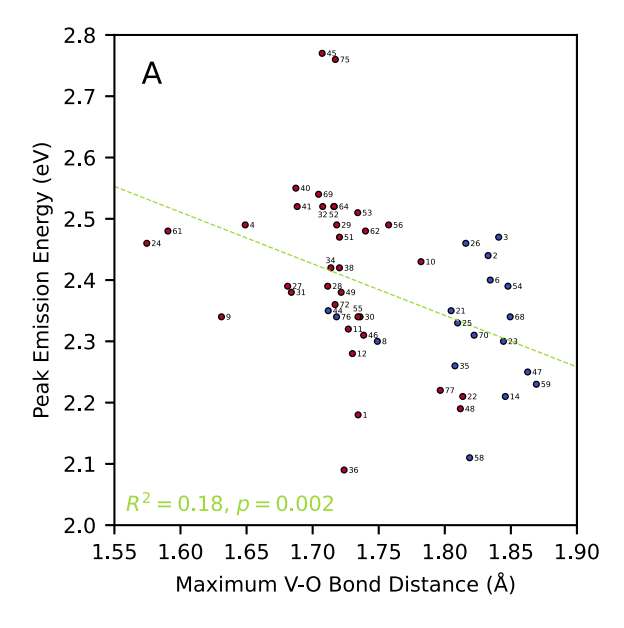
# 3.2.2. Hole localisation

It is interesting to check whether evidence of localisation of the hole on a single oxygen atom can be found within the emission spectra. We expect that the localisation of the hole on one or more oxygen atoms leads to expansion of their concomitant V-O bond to minimise the energy of the system. Then, when the VO<sub>4</sub> centres already have a lower symmetry than  $\mathbf{T}_d$  in the ground state (as is often the case), we expect that the hole would be localised on the oxygen atom with the largest V-O bond length. It has also been suggested that the length of the V-O bond and the emission energy are negatively correlated [142]. Therefore, if the localisation of the hole on the longest V-O bond is generally the case, then a correlation between the maximum V-O bond length and emission energy would be expected.

At first sight, our results give some indication of this. The correlation between the maximum length of the V-O bond and the emission energy appears significant (p = 0.002) while the correlation between the average length of the V-O bond and the peak emission energy is not significant (p = 0.11), respectively, shown in Figs. 8A and 8B. However, it is noticeable that the vanadates with the highest maximum V-O bond length are also those in which the VO<sub>4</sub> centres form dimers, trimers or chains (coloured blue in Fig. 8) instead of being isolated (coloured red). Therefore, it could also be the case that the connectivity between the VO<sub>4</sub> centres plays a role, rather than the maximum V-O bond length. Together with the low coefficient of determination, no conclusive remarks about the localisation of hole based on the emission spectra can be made.

## 3.2.3. Free exciton emission

In some rare cases, at cryogenic temperatures, sharp exciton emission can be observed in vanadate compounds in addition to their typical broad emission [143]. Previously, the broadband feature was attributed



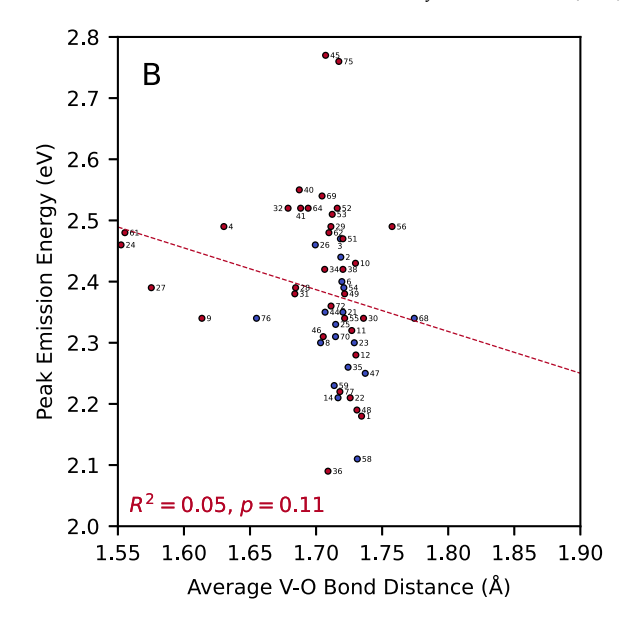


**Fig. 8.** A) Energy of the maximum in the emission spectrum against the maximum distance between oxygen and vanadium in the vanadate group. The red datapoints are of orthovanadates, the blue datapoints are vanadates with higher connectivity; dimers, trimers or chains. The green dashed line shows a linear fit with  $R^2 = 0.18$ , p = 0.002, indicating a statistically significant correlation. B) Energy of the maximum in the emission spectrum against the mean distance between oxygen and vanadium in the vanadate group. The red dashed line shows a linear fit with  $R^2 = 0.05$ , p = 0.11, indicating no statistically significant correlation.

to defect emission [143,144]. It should be noted that  $CsVO_3$ , in which this exciton emission has been observed, has an IQY close to unity [43]. We find the attribution of defects to the broad luminescence band of  $CsVO_3$  improbable, as with few exceptions, defects often lead to quenching rather than efficient emission, and as the excitation and emission spectra, as well as the excited-state lifetime, are similar to those of other vanadates. Rather, we propose that free exciton emission in vanadates can now also be understood from the mechanism of luminescence initiated with polaron formation; According to the Mott and Stoneham model, polaron formation can have an activation barrier [145,146], and due to this barrier, photogenerated delocalised carriers have a sufficient lifetime at low temperatures to result in observable free exciton emission.

# 3.2.4. Overview hypothesis

In summary, we hypothesise that the description of the mechanism of excitation and luminescence as localised CT transitions in the VO<sub>4</sub> centre described by molecular orbital theory is incorrect. Rather, the excitation has a delocalised nature. It is a bandgap excitation that results in the formation of free charge carriers. Then, the electrons rapidly localise on V<sup>5+</sup>, forming electron polarons. Subsequently, the holes combine with the electron polarons to form self-trapped excitons. Possibly, in these self-trapped excitons, the hole wavefunction localises on the oxygen atom most distant from the central vanadium atom. This trapping is accompanied by a significant distortion of the centre in which the V-O bond with the hole becomes elongated. The emission then results from the recombination of the self-trapped excitons.

Such a mechanism can explain the large variation in the energetic position of the excitation spectra among compounds, its comparatively weak dependence on the maximum emission wavelength, the observation of delayed  $\rm V^{4+}$  formation, the strong localised character of the excited state accompanied with deformations of the  $\rm VO_4$  tetrahedron measured and predicted in EPR and *ab initio* studies, and the co-existence of sharp free-exciton and broad emission.

# 3.3. The suggested structure-efficiency relations

For many applications of phosphors, the luminescence efficiency is of utmost importance. The origin of quenching can be categorised into two types: nonradiative decay within a luminescent centre, which we will refer to as thermal quenching, and nonradiative decay induced by neighbouring lattice defects, which we will refer to as defect quenching. Note that the degree of defect quenching can also increase with temperature due to the possibility of thermally assisted migration of the excitation, as is the case for vanadates [134]. If the origin of quenching is by defects, then the phosphor is not intrinsically limited to have a low IQY and there is room for improvement by optimisation of the synthesis conditions to lower the amount of defects, or by decreasing the mobility of the excited state by lowering the amount of activators between which migration can occur. In contrast, if the origin is thermal quenching, the IQY is intrinsically limited and cannot be improved without changing the composition of the host lattice. The quenching models proposed by Blasse and Nakajima, both forms of thermal quenching, have commonly been used to explain quenching in vanadates. We will describe these models and test their validity with data from literature.

## 3.3.1. Blasse's hypothesis on internal quenching

Following the Mott-Seitz model of luminescence [147], the rate of thermal quenching is exponentially dependent on the energy of a single activation barrier to transition from the excited state to the ground state through a crossover point. If the activation barrier is sufficiently low, nonradiative relaxation via the crossover point becomes dominant over radiative relaxation, resulting in a low IQE. As the activation barrier for thermal quenching decreases with the decreasing position of the absorption band edge, the temperature at which thermal quenching becomes significant, the quenching temperature, should decrease with decreasing position of the absorption band. Blasse noted that this general relationship applies to d0-ions with 6-fold coordination, such as  $W^{6+}$  in  $[WO_6]^{6-}$ , but fails for those with 4-fold coordination [148]. In agreement, we also found that there is no relationship between the peak excitation energy and the IQY for the vanadates (see Figure S1). As charge transfer transitions are accompanied by significant lattice relaxation, the change in configurational coordinate, also called the Frank-Condon (FC) offset, is also large [1]. For some d0-tetroxo-ions, such as [WO<sub>4</sub>]<sup>2-</sup>, the FC offset can be sufficiently large and the excitation energy sufficiently low, so that the energy of the crossover point is lower than the excitation energy (the Dexter-Klick-Russell model) and, as a consequence, quenching does not require phonons [149,150]. As the FC offset and activation barrier for thermal quenching are negatively correlated, Blasse suggested that vanadate groups would be able to lu-

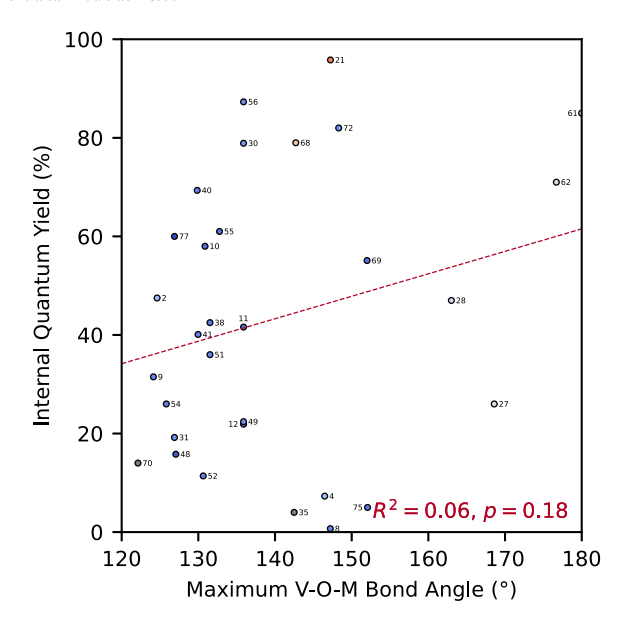


**Fig. 9.** Internal quantum yield against the highest angle between the V-O bond and the O-M bond. The mean polarizability of the cations (excluding vanadium) was calculated and is indicated with the colours blue (low polarizability) to red (high polarizability). The red dashed line shows a linear fit with  $R^2 = 0.06$ , p = 0.18, indicating no statistically significant correlation.

minescence efficiently if they were incorporated into a stiff lattice [2,5], similar to what had been observed for many other luminescent centres [151]. A stiff lattice would resist the relaxation of the lattice accompanying the electronic transitions in the  $VO_4$  centre, thereby decreasing the FC offset of the luminescent state and increasing the activation barrier, which in turn results in a higher IQE. Blasse defined stiff lattices as those composed of ions with low polarisability, i.e. those with small ionic radii and high oxidation states. Furthermore, since it was expected that the relaxation of the lattice occurred predominantly by expansion of the V-O bond, he suggested that crystal structures in which ions with low polarisability lie on the produced part of the V-O bond, that is, an angle of the V-O-M bond close to  $180^\circ$ , would prevent thermal quenching. Examples of phosphors that meet these criteria are  $YVO_4$  and  $SiO_2:V^{5+}$ .

However, as shown in Fig. 9, there appears to be no correlation between the quantum efficiency and the max. V-O-M bond angle. Although it is difficult to capture the polarisability of the atoms surrounding the VO<sub>4</sub> centres in a single number, the mean polarisability of the cations (excluding vanadium) was calculated and is indicated with the colours blue (low polarisability) to red (high polarisability) in Fig. 9. In contrast to Blasse's prediction, vanadate phosphors with the highest IQY are those with highly polarisable ions such as Rb<sup>+</sup> and Cs<sup>+</sup>. In fact, in the series of alkali vanadates MVO3, no luminescence is often reported for  ${\rm LiVO_3}$ , the "stiffest" of these lattices, and it increases sharply across the series from NaVO<sub>3</sub> to CsVO<sub>3</sub> [4,7]. Note that the crystal structure does not change significantly in these series [152]. Similar trends have been observed in other series of alkali vanadates [7], see Fig. 10. Given the absence of a correlation between the V-O-M bond angle and the internal quantum yield, as well as the observation that luminescence efficiency is generally higher for compounds containing highly polarizable ions, we conclude that high lattice stiffness is not a reliable criterion for efficient luminescence in vanadates.

Blasse also predicted that the stiffness of the lattice would influence the width and emission of the emission spectrum. As the stiffness of the lattices increases, the FC offset of the luminescent state is expected to decrease, and should therefore generally be accompanied by a decreasing width and increasing peak emission energy of the emission spectrum. Note that normally the Stokes shift should decrease, but as the electronic states for excitation and emission are expected to be different, the use of the peak emission energy is more appropriate. Although we did find

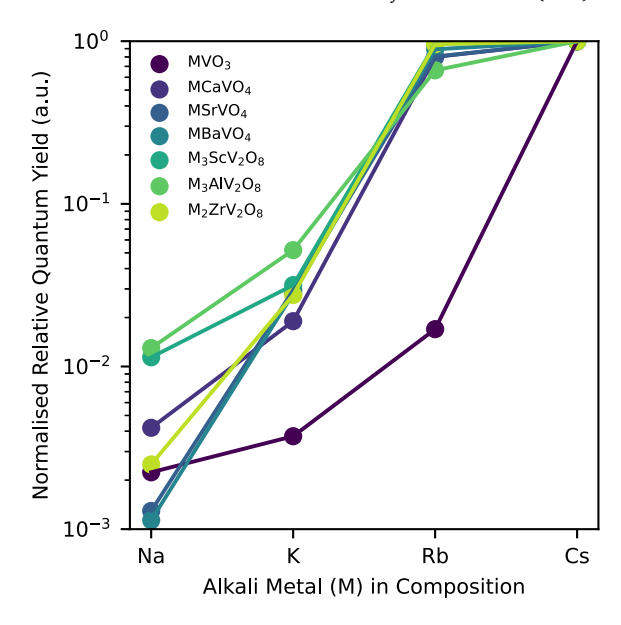


**Fig. 10.** Internal quantum yield of alkali vanadate phosphors as function of the alkali metal in the composition, relative to that of the Cs containing phosphor [7].

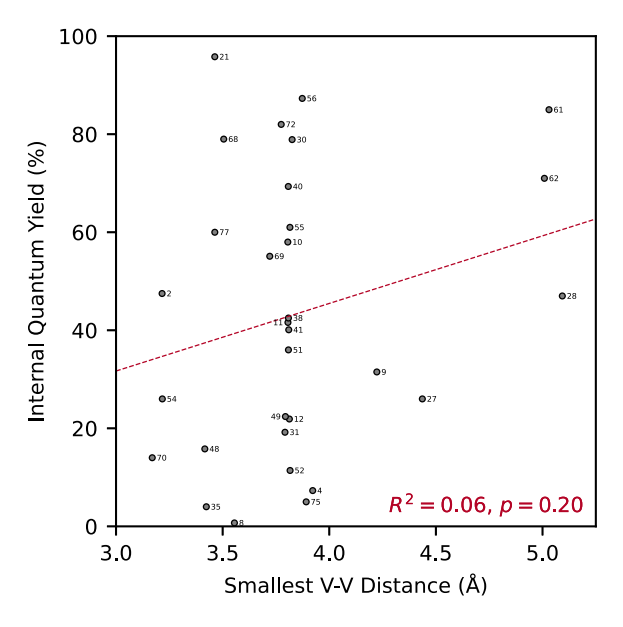


**Fig. 11.** Internal quantum yield against the smallest distance between two vanadium atoms. The red dashed line shows a linear fit with  $R^2 = 0.06$ , p = 0.20, indicating no statistically significant correlation.

a statistically significant relation between the max. V-O-M bond angle and the peak emission energy (see Figure S2), we did not for the max. V-O-M bond angle and emission width (see Figure S3). It is noticeable that lattices with a high max. V-O-M angles, namely  $K_3LaV_2O_8$ ,  $Rb_3LuV_2O_8$ , and  $Zn_2V_2O_7$ , with respectively  $La^{3+}$ ,  $Y^{3+}$ ,  $Lu^{3+}$  and  $Zn^{2+}$  on the produced part of the V-O bonds, have below average width, in line with Blasse's prediction. However, many lattices that consist of highly polarisable atoms and have a relatively low max. V-O-M bond angles also show relatively high energy and low width of emission. In light of these observations, we tentatively conclude that Blasse's description of the stiffness of the vanadate group is not a reliable predictor of the FC offset, the energy of the emitting state, and the degree of quenching.

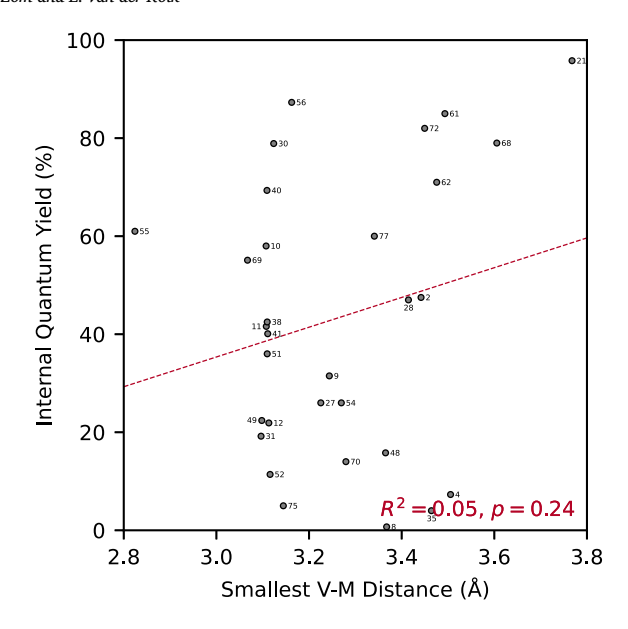


**Fig. 12.** Internal quantum yield against the smallest distance between a vanadium atom and another cation. The red dashed line shows a linear fit with  $R^2 = 0.05$ , p = 0.24, indicating no statistically significant correlation.

### 3.3.2. Nakajima's hypothesis on internal quenching

Nakajima et al. measured the quantum yield of vanadate oxides,  $M^+VO_3$ ,  $M_2^{2+}V_2O_7$  and  $M_3^{2+}V_2O_8$  ( $M^+$  = Li, Na, K, Rb, and Cs;  $M^{2+}$  = Mg, Ca, Sr, Ba, and Zn) and analysed their crystalline properties [4]. They suggested that IQY increases with decreasing separation between vanadium atoms and with increasing separation between the vanadium atoms and other cations. They explained their results by hypothesising that "strong V-V interactions" and "weak M-V interactions" are required to obtain a high IQY. To support their hypothesis, they suggested a mechanism in which "strong V-V interactions" and "weak M-V interactions" lead to enhanced exciton diffusion. They also hypothesized that such enhanced exciton diffusion leads to a longer lifetime of the singlet states, and that there is an activation barrier for the transition from the singlet states to the triplet states, which can be reduced by dynamic Jahn-Teller distortions. A long singlet lifetime can then facilitate intersystem crossing. As they propose nonradiative relaxation occurs from the singlet states, enhanced intersystem crossing, in turn, increases the IQY. This model was put forth by Nakajima and has often been used to explain differences among compounds and even synthesis conditions.

In Figs. 11 and 12, we show the IQY as a function of, respectively, the smallest V-V and M-V distance. From these figures, it is evident that there are no clear relationships between these properties and the IQY. Furthermore, if dynamic Jahn-Teller distortions, and thereby phonons, are required to facilitate intersystem crossing, then the luminescence of vanadates should be phonon-assisted. However, such a rise of the luminescence intensity with increasing temperature is rarely observed. Rather, the luminescence efficiency is often reported to decrease monotonically with increasing temperature [5].

# 4. Conclusions

By analysing past experimental research, we have demonstrated that excitations in vanadate phosphors are unlikely to be localised charge-transfer transitions, in contrast to the established luminescent mechanism. Rather, based on the broad character of the excitation spectra, the absence of a correlation between the excitation spectrum and VO<sub>4</sub> structure, and the strong influence of the host composition on the excitation spectrum, we hypothesise that excitations are interband excitations. Furthermore, based on the observation of delayed V<sup>4+</sup> formation and various EPR and *ab initio* studies, we hypothesise that free electrons are capable of forming small polarons localised on V<sup>5+</sup> and subsequently

form self-trapped excitons, which are responsible for broad and Stokesshifted luminescence. By analysing luminescent characteristics against structural properties, we also demonstrated that there is no strong evidence for the two mechanisms proposed by Blasse and Nakajima, which are often used to explain quenching in vanadate phosphors.

## CRediT authorship contribution statement

**Jeffrey Zom:** Writing – original draft, Validation, Methodology, Formal analysis, Writing – review & editing, Visualization, Software, Investigation, Data curation. **Erik van der Kolk:** Validation, Resources, Funding acquisition, Writing – review & editing, Supervision, Project administration.

## **Funding**

This work was supported by the Netherlands Organisation for Scientific Research (NWO) under project number ENPPS.TA.019.007.

## **Declaration of competing interest**

The authors declare that they have no known competing financial interests or personal relationships that could have appeared to influence the work reported in this paper.

## Appendix A. Supplementary material

Supplementary material related to this article can be found online at https://doi.org/10.1016/j.jlumin.2025.121397.

## Data availability

Data will be made available on request.

# References

- G. Blasse, The Luminescence of Closed-Shell Transition-Metal Complexes. New Developments, Luminescence and Energy Transfer. Structure and Bonding, vol. 42, Springer, Berlin, Heidelberg, 1980, pp. 1–41.
- [2] G. Blasse, Classical phosphors: a Pandora's box, J. Lumin. 72–74 (1997) 129–134, https://doi.org/10.1016/S0022-2313(96)00166-4.
- [3] J. Van Tol, J.H. Van Der Waals, The luminescent triplet state of VO<sub>4</sub><sup>3-</sup> in YPO<sub>4</sub>, Mol. Phys. 76 (3) (1992) 567–590, https://doi.org/10.1080/00268979200101541.
- [4] T. Nakajima, et al., Correlation between luminescence quantum efficiency and structural properties of vanadate phosphors with chained, dimerized, and isolated VO<sub>4</sub> tetrahedra, J. Phys. Chem. C 114 (11) (2010) 5160–5167, https:// doi.org/10.1021/jp910884c.
- [5] H. Ronde, G. Blasse, The nature of the electronic transitions of the vanadate group,
   J. Inorg. Nucl. Chem. 40 (2) (1978) 215–219, https://doi.org/10.1016/0022-1902(78)80113-4.
- [6] C.J. Ballhausen, A.D. Liehr, Intensities in inorganic complexes: part II. Tetrahedral complexes, J. Mol. Spectrosc. 2 (1–6) (1958) 342–360, https://doi.org/10.1016/ 0022-2852(58)90086-9.
- [7] A.A. Fotiev, et al., Vanadium Crystallophosphors: Synthesis and Properties, Publishing House "Nauka", Moscow, USSR, 1976.
- [8] R. Enjalbert, J. Galy, A refinement of the structure of V<sub>2</sub>O<sub>5</sub>, Acta Crystallogr., Sect.
   C 42 (11) (1986) 1467–1469, https://doi.org/10.1107/S0108270186091825.
- [9] Y. Oka, T. Yao, N. Yamamoto, Hydrothermal synthesis and structure refinements of alkali-metal trivanadates AV<sub>3</sub>O<sub>8</sub> (A = K, Rb, Cs), Mater. Res. Bull. 32 (9) (1997) 1201–1209.
- [10] V.K. Trunov, et al., Crystalline structure of calcium pyrovanadate, Dokl. Akad. Nauk SSSR 270 (4) (1983) 886–887.
- [11] G.A. Karim, U.R.K. Rao, R. Prasad, Synthesis and cell dimensions of ReBa<sub>2</sub>VO<sub>6</sub>-type compounds, where Re = rare earth, J. Mater. Sci. Lett. 7 (1988) 1239–1240, https://doi.org/10.1007/BF00722349.
- [12] B.N. Parida, et al., Ferroelectric and optical modulations of double perovskite Ba<sub>2</sub>BiVO<sub>6</sub>, J. Mol. Struct. 1189 (5) (2019) 288–298, https://doi.org/10.1016/j. molstruc.2019.04.043.
- [13] L.K. Bharat, K.G. Krishna, J.S. Yu, Effect of transition metal ion (Nb<sup>5+</sup>) doping on the luminescence properties of self-activated Ca<sub>2</sub>AgZn<sub>2</sub>V<sub>3</sub>O<sub>12</sub> phosphors, J. Alloys Compd. 699 (30) (2017) 756–762, https://doi.org/10.1016/j.jallcom.2016.12. 385

- [14] Y. Matsushima, et al., Self-activated vanadate compounds toward realization of rare-earth-free full-color phosphors, J. Am. Ceram. Soc. 98 (4) (2015) 1236–1244, https://doi.org/10.1111/jace.13463.
- [15] P. Kaur, A. Khanna, Structural, electrical and luminescence properties of M<sub>2</sub>V<sub>2</sub>O<sub>7</sub> (M = Mg, Ca, Sr, Ba, Zn), J. Mater. Sci., Mater. Electron. 32 (2021) 21813–21823, https://doi.org/10.1007/s10854-021-06710-y.
- [16] N. Kaczorowska, et al., Synthesis and luminescence tunability studies in new upconverting Ba<sub>2</sub>V<sub>2</sub>O<sub>7</sub> phosphors, Polyhedron 223 (1) (2022) 115940, https:// doi.org/10.1016/j.poly.2022.115940.
- [17] M. Takahashi, M. Hagiwara, S. Fujihara, Liquid-phase synthesis of Ba<sub>2</sub>V<sub>2</sub>O<sub>7</sub> phosphor powders and films using immiscible biphasic organic-aqueous systems, Inorg. Chem. 55 (16) (2016) 7879–7885, https://doi.org/10.1021/acs.inorgchem. 6b00716
- [18] R. Yu, et al., Preparation, structure and luminescence properties of Ba<sub>2</sub>V<sub>2</sub>O<sub>7</sub> microrods, RSC Adv. 6 (93) (2016) 90711–90717, https://doi.org/10.1039/ C6RA17072B
- [19] N.V. Bharathi, et al., Synthesis and characterization of self-activated Ba<sub>2</sub>V<sub>2</sub>O<sub>7</sub> nanophosphor: a potential material for W-LED applications, Mater. Res. Express 6 (10) (2019) 106202, https://doi.org/10.1088/2053-1591/ab3c1d.
- [20] N. Wang, et al., Syntheses and characterization of a family of vanadate compounds  $Ba_3M(V_2O_7)_2$  (M = Co, Mn, Mg, or Zn) with an edge-shared  $[M_2O_{10}]$  dimer structure, Cryst. Growth Des. 15 (4) (2015) 1619–1624, https://doi.org/10.1021/cg5012814.
- [21] L. Krishna Bharat, et al., Sol-gel derived barium orthovanadate phosphors for white light-emitting diodes, Dyes Pigments 150 (2018) 44–48, https://doi.org/10.1016/ j.dyepig.2017.11.006.
- [22] K.-C. Park, S.-i. Mho, Photoluminescence properties of  $Ba_3V_2O_8$ ,  $Ba_{3(1-x)}Eu_2xV_2O_8$  and  $Ba_2Y_{2/3}V_2O_8$ :  $Eu_{3+}$ , J. Lumin. 122–123 (2007) 95–98, https://doi.org/10.1016/j.jlumin.2006.01.107.
- [23] M. Xin, et al., Luminescence properties of self-activated M<sub>3</sub>(VO<sub>4</sub>)<sub>2</sub> (M = Mg, Ca, Sr and Ba) phosphors synthesized by solid-state reaction method, J. Nanosci. Nanotechnol. 16 (4) (2016) 3684–3689, https://doi.org/10.1166/jnn.2016.11825.
- [24] K.-C. Park, et al., New luminescent materials: Ba $_3V_2O_8$  and Ba $_2V_{2/3}V_2O_8$ :Eu $^{3+}$ , Soc. Inf. Disp. 36 (1) (2005) 583–585, https://doi.org/10.1889/1.2036506.
- [25] S. Shisina, et al., Structure and optoelectronic properties of palmierite structured  $Ba_2Y_{0.67}\delta_{0.33}V_2O_8$ : Eu<sup>3+</sup> red phosphors for n-UV and blue diode-based warm white light systems, J. Alloys Compd. 802 (2019) 723–732, https://doi.org/10.1016/j. iallcom.2019.05.355.
- [26] R. Singh, S.J. Dhoble, Photoluminescence property of A<sub>9</sub>B(VO<sub>4</sub>)<sub>7</sub> [A = Ca, Sr, Ba and B = La, Gd] phosphors, Luminescence 28 (4) (2013) 607–611, https://doi.org/10.1002/bio.2407.
- [27] R. Yu, J.H. Jeong, Y.-F. Wang, A novel Eu<sup>3+</sup>- and self-activated vanadate phosphor of Ca<sub>4</sub>La(VO<sub>4</sub>)<sub>3</sub>O with oxyvanadate apatite structure, J. Am. Ceram. Soc. 100 (12) (2017) 5649–5658, https://doi.org/10.1111/jace.15102.
- [28] H. He, et al., Luminescence properties of self-activated  $Ca_5Mg_3Zn(VO_4)_6$  and  $Ca_5Mg_3Zn(VO_4)_6$ :xEu<sup>3+</sup> phosphors, Luminescence 36 (2) (2021) 316–325, https://doi.org/10.1002/bio.3943.
- [29] J.Y. Park, J.W. Chung, H.K. Yang, Synthesis and photoluminescence properties of yellow-emitting  $Ca_5(Zn_{1-x}Mg_x)_4(VO_4)_6$  self-activated phosphors, Optik 155 (2018) 384–389, https://doi.org/10.1016/j.ijleo.2017.11.046.
- [30] N. Zhang, et al., A vanadate-based white light emitting luminescent material for temperature sensing, RSC Adv. 9 (52) (2019) 30045–30051, https://doi.org/10. 1039/C9RA06193B.
- [31] Z. Liu, et al., Highly efficient rare-earth free vanadate phosphors for WLEDs, Dalton Trans. 52 (45) (2023) 16819–16828, https://doi.org/10.1039/D3DT03138A.
- [32] Y. Huang, et al., Novel yellow-emitting phosphors of Ca<sub>5</sub>M<sub>4</sub>(VO<sub>4</sub>)<sub>6</sub> (M = Mg, Zn) with isolated VO<sub>4</sub> tetrahedra, Opt. Express 20 (4) (2012) 4360–4368, https://doi.org/10.1364/OF.20.004360.
- [33] E. Pavitra, et al., Novel rare-earth-free yellow Ca<sub>5</sub>Zn<sub>3,92</sub>In<sub>0.08</sub>(V<sub>0.99</sub>Ta<sub>0.01</sub>O<sub>4</sub>)<sub>6</sub> phosphors for dazzling white light-emitting diodes, Sci. Rep. 5 (2015) 10296, https://doi.org/10.1038/srep10296.
- [34] V.G. Zubkov, et al., Synthesis, crystal structure and luminescent properties of pyrovanadates A<sub>2</sub>CaV<sub>2</sub>O<sub>7</sub> (A = Rb, Cs), Solid State Sci. 11 (3) (2009) 726–732, https://doi.org/10.1016/j.solidstatesciences.2008.09.009.
- [35] B.V. Slobodin, et al., Thermochemical and luminescent properties of the K<sub>2</sub>MgV<sub>2</sub>O<sub>7</sub> and M<sub>2</sub>CaV<sub>2</sub>O<sub>7</sub> (M = K, Rb, Cs) vanadates, Inorg. Mater. 46 (2010) 522–528, https://doi.org/10.1134/S0020168510050158.
- [36] B.V. Slobodin, et al., Thermal and luminescent properties of M<sub>2</sub>Zn(VO<sub>3</sub>)<sub>4</sub> (M = Rb, Cs), Inorg. Mater. 49 (2013) 834–838, https://doi.org/10.1134/S0020168513080165.
- [37] T. Li, et al., Photoluminescence Characterization of Zn- and Cs-Vanadate Phosphors, in: Proceedings of 2nd International Conference on Photonics, Optics and Laser Technology 1, 2014, pp. 63–65.
- [38] Y. Pu, et al., An efficient yellow-emitting vanadate Cs<sub>5</sub>V<sub>3</sub>O<sub>10</sub> under UV light and X-ray excitation, Mater. Lett. 149 (2015) 89–91, https://doi.org/10.1016/j.matlet. 2015.02.108.
- [39] Y. Pu, et al., Intrinsic [VO<sub>4</sub>]<sup>3-</sup> emission of cesium vanadate  $Cs_5V_3O_{10}$ , RSC Adv. 5 (90) (2015) 73467–73473, https://doi.org/10.1039/c5ra11823a.
- [40] B.V. Slobodin, et al., Preparation and luminescent properties of rubidium and cesium vanadates, Inorg. Mater. 50 (2014) 179–183, https://doi.org/10.1134/ S0020168514020150.

- [41] H. Gobrecht, G. Heinsohn, On the luminescence of alkali vanadates, Z. Phys. 147 (1957) 350–360, https://doi.org/10.1007/BF01333104.
- [42] A.V. Ishchenko, et al., Luminescence mechanism and energy transfer in cesium metavanadate CsVO<sub>3</sub>, Radiat. Meas. 124 (2019) 48–53, https://doi.org/10.1016/ i.radmeas.2019.03.003.
- [43] T. Nakajima, et al., Rare earth-free high color rendering white light-emitting diodes using  $CsVO_3$  with highest quantum efficiency for vanadate phosphors, J. Mater. Chem. C 3 (41) (2015) 10748–10754, https://doi.org/10.1039/C5TC01929J.
- [44] X. Qiao, et al., Preparation, characterization and high quantum efficiency of yellow-emitting CsVO<sub>3</sub> nanofibers, J. Alloys Compd. 656 (2016) 843–848, https://doi.org/10.1016/j.jallcom.2015.10.022.
- [45] T. Nakajima, et al., Direct fabrication of metavanadate phosphor films on organic substrates for white-light-emitting devices, Nat. Mater. 7 (2008) 735–740, https://doi.org/10.1038/nmat2244.
- [46] E. Pavitra, et al., Evolution of highly efficient rare-earth free Cs<sub>(1-x)</sub>Rb<sub>x</sub>VO<sub>3</sub> phosphors as a single emitting component for NUV-based white LEDs, J. Mater. Chem. C 6 (46) (2018) 12746–12757, https://doi.org/10.1039/C8TC05110K.
- [47] H.-R. Shih, et al., Synthesis and photoluminescence properties of (La, Pr) co-doped InVO<sub>4</sub> phosphor, Microelectron. Eng. 148 (2015) 10–13, https://doi.org/10.1016/ i.mee.2015.07.007.
- [48] J. Shen, et al., Synthesis and characterization of InVO<sub>4</sub> nano-materials and their photoluminescence properties, Proc. Eng. 94 (2014) 64–70, https://doi.org/10. 1016/j.proeng.2013.11.043.
- [49] P. Botella, et al., Investigation on the luminescence properties of InMO<sub>4</sub> (M = V<sup>5+</sup>, Nb<sup>5+</sup>, Ta<sup>5+</sup>) crystals doped with Tb<sup>3+</sup> or Yb<sup>3+</sup> rare earth ions, ACS Omega 5 (5) (2020) 2148–2158, https://doi.org/10.1021/acsomega.9b02862.
- [50] G. Blasse, A. Bril, Luminescence of phosphors based on host lattices ABO<sub>4</sub> (A is Sc, In B is P, V, Nb), J. Chem. Phys. 50 (7) (1969) 2974–2980, https://doi.org/10.1063/1.1671493.
- [51] R. Van de Krol, J. Ségalini, C.S. Enache, Influence of point defects on the performance of InVO<sub>4</sub> photoanodes, J. Photon. Energy 1 (1) (2011) 016001, https://doi.org/10.1117/1.3564926.
- [52] A.D.J. David, G.S. Muhammad, V. Sivakumar, Synthesis and optical properties of Eu<sup>3+</sup>-substituted glaserite-type orthovanadates CsK<sub>2</sub>Y[VO<sub>4</sub>]<sub>2</sub>, Luminescence 32 (5) (2017) 735–744, https://doi.org/10.1002/bio.3244.
- [53] J. Sonawane, et al., A novel self-activated K<sub>2</sub>XV<sub>2</sub>O<sub>7</sub> (X = Mg and Zn) pyrovanadate green phosphor: Systematic characterization and time-resolved photoluminescence, Solid State Sci. 61 (2016) 207–214, https://doi.org/10.1016/j.solidstatesciences.2016.10.004.
- [54] L. Qin, et al., Ortho-vanadates  $K_3$ RE(VO<sub>4</sub>)<sub>2</sub> (RE = La, Pr, Eu, Gd, Dy, Y) for near UV-converted phosphors, Mater. Chem. Phys. 147 (3) (2014) 1195–1203, https://doi.org/10.1016/j.matchemphys.2014.07.006.
- [55] X. Huang, et al., KCa<sub>2</sub>Mg<sub>2</sub>V<sub>3</sub>O<sub>12</sub>: A novel efficient rare-earth-free self-activated yellow-emitting phosphor, J. Photochem. Photobiol. A, Chem. 401 (2020) 112765, https://doi.org/10.1016/j.jphotochem.2020.112765.
- [56] J. Xie, et al., Structure and luminescence characteristics of self-activated vanadate garnet phosphors, Phys. Chem. Chem. Phys. 26 (38) (2024) 25048–25056, https://doi.org/10.1039/D4CP03074E.
- [57] L. Yang, et al., Tunable luminescence and energy transfer properties in  $Ca_{2-x}NaMg_2V_3O_{12}:xEu^{3+}$  phosphors, J. Mater. Sci., Mater. Electron. 28 (2017) 9975–9982, https://doi.org/10.1007/s10854-017-6779-8.
- [58] J. Li, et al., A novel broadband emission phosphor Ca<sub>2</sub>KMg<sub>2</sub>V<sub>3</sub>O<sub>12</sub> for white light emitting diodes, Mater. Res. Bull. 45 (5) (2010) 598–602, https://doi.org/10.1016/ i.materresbull.2010.01.014.
- [59] H. Xie, et al., Luminescence and quantum efficiencies of Eu<sup>3+</sup>-doped vanadate garnets, J. Am. Ceram. Soc. 97 (5) (2014) 1434–1441, https://doi.org/10.1111/jace. 12771.
- [60] L.K. Bharat, et al., Rare-earth free self-luminescent Ca<sub>2</sub>KZn<sub>2</sub>(VO<sub>4</sub>)<sub>3</sub> phosphors for intense white light-emitting diodes, Sci. Rep. 7 (2017) 42348, https://doi.org/10. 1038/srep42348.
- [61] T. Jeyakumaran, et al., Facile synthesis, vibrational, optical and improved luminescence properties analysis of Ca<sub>2</sub>KZn<sub>2</sub>V<sub>3</sub>O<sub>12</sub> phosphor, Mater. Res. Express 6 (2019) 116329, https://doi.org/10.1088/2053-1591/ab51b8.
- [62] M. Colmont, et al., On the use of dynamical diffraction theory to refine crystal structure from electron diffraction data: application to  $KLa_5O_5(VO_4)_2$ , a material with promising luminescent properties, Inorg. Chem. 55 (5) (2016) 2252–2260, https://doi.org/10.1021/acs.inorgchem.5b02663.
- [63] Y. Xiang, et al., Ultra-broadband emission up to 181 nm of VO<sub>4</sub>-activated yellow phosphor for white light-emitting diodes with high color rendering index, J. Lumin. 267 (2024) 120397, https://doi.org/10.1016/j.jlumin.2023.120397.
- [64] O.V. Chukova, et al., Synthesis and properties of the  $La_{1-x-y}Eu_yCa_xVO_4$  ( $0 \le x, y \le 0.2$ ) compounds, Nanoscale Res. Lett. 12 (2017), https://doi.org/10.1186/s11671-017-2116-7.
- [65] A. Princy, et al., Greenish-yellow luminescence in vanadate garnet phosphors: structural characterization, energy transfer and Judd-Ofelt analysis of Dy<sup>3+</sup>-Doped Ca<sub>2</sub>LiMg<sub>2</sub>V<sub>3</sub>O<sub>12</sub>, J. Inorg. Organomet. Polym. Mater. 33 (2023) 2399–2410, https://doi.org/10.1007/s10904-023-02687-9.
- [66] J. Zhou, et al., Synthesis, energy transfer and multicolor luminescent property of  ${\rm Eu}^{3+}$ -doped  ${\rm LiCa_2Mg_2V_3O_{12}}$  phosphors for warm white light-emitting diodes, Ceram. Int. 45 (11) (2019) 13832–13837, https://doi.org/10.1016/j.ceramint.2019. 04.080.

- [67] H. Chen, et al., Broad-band emission and color tuning of Eu<sup>3+</sup>-doped LiCa<sub>2</sub>Sr-MgV<sub>3</sub>O<sub>12</sub> phosphors for warm white light-emitting diodes, Opt. Mater. 89 (2019) 132–137, https://doi.org/10.1016/j.optmat.2019.01.012.
- [68] G. Warutkar, et al., Host-sensitized mid-infrared emission in LiCa<sub>3</sub>MgV<sub>3</sub>O<sub>12</sub> activated with Er<sup>3+</sup>, Emerg. Mater. 8 (2024) 751–757, https://doi.org/10.1007/s42247-024-00819-6.
- [69] H. Zhou, et al., Novel ratiometric optical thermometry based on dual luminescent centers from europium doped LiCa<sub>3</sub>MgV<sub>3</sub>O<sub>12</sub> phosphor, Ceram. Int. 45 (13) (2019) 16651–16657, https://doi.org/10.1016/j.ceramint.2019.05.207.
- [70] X. Huang, H. Guo, A novel highly efficient single-composition tunable white-light-emitting  $\text{LiCa}_3\text{MgV}_3\text{O}_{12}$ : $\text{Eu}^{3+}$  phosphor, Dyes Pigments 154 (2018) 82–86, https://doi.org/10.1016/j.dyepig.2018.02.047.
- [71] Y. Lv, et al., Synthesis and luminescence studies of mixed-phase  $LiGa_3MgV_{3-x}W_xO_{12}$  phosphors for enhanced quantum yield, J. Lumin. 234 (2011) 117948, https://doi.org/10.1016/j.jlumin.2021.117948.
- [72] Y. Lv, et al., Role of oxygen vacancy in rare-earth-free LiCa<sub>3</sub>Mg(VO<sub>4</sub>)<sub>3</sub> phosphor: enhancing photoluminescence by heat-treatment in oxygen flow, J. Mater. Sci. Technol. 79 (2021) 123–132, https://doi.org/10.1016/j.jmst.2020.11.039.
- [73] R. Cao, et al., Tunable emission of LiCa<sub>3</sub>MgV<sub>3</sub>O<sub>12</sub>:Bi<sup>3+</sup> via energy transfer and changing excitation wavelength, Mater. Res. Bull. 111 (2019) 87–92, https://doi.org/10.1016/j.materresbull.2018.11.011.
- [74] T. Hasegawa, et al., Bluish-white luminescence in rare-earth-free vanadate garnet phosphors: structural characterization of LiCa<sub>3</sub>MV<sub>3</sub>O<sub>12</sub> (M = Zn and Mg), Inorg. Chem. 57 (2) (2017) 857–866, https://doi.org/10.1021/acs.inorgchem.7b02820.
- [75] M. Zhu, Q. Ma, N. Guo, Optical thermometry based on europium doped self-activated dual-emitting LiCa<sub>3</sub>ZnV<sub>3</sub>O<sub>12</sub> phosphor, Spectrochim. Acta, Part A, Mol. Biomol. Spectrosc. 271 (2022) 120922, https://doi.org/10.1016/j.saa.2022. 120922
- [76] H. Jiao, et al., Color-tunable single-phase Bi<sup>3+</sup>/Eu<sup>3+</sup>-activated LiCa<sub>3</sub>ZnV<sub>3</sub>O<sub>12</sub> luminescence materials based on energy transfer, ChemistrySelect 7 (33) (2022) 202203046, https://doi.org/10.1002/slct.202203046.
- [77] X. Zhang, et al., Host-sensitized color-tunable luminescence properties of self-activated and Eu<sup>3+</sup>-doped Ca<sub>3</sub>LiZnV<sub>3</sub>O<sub>12</sub> phosphors, J. Lumin. 203 (2018) 735–740, https://doi.org/10.1016/j.jlumin.2018.07.030.
- [78] X. Huang, H. Guo, Synthesis and photoluminescence properties of Eu<sup>3+</sup>-activated LiCa<sub>3</sub>ZnV<sub>3</sub>O white-emitting phosphors, RSC Adv. 8 (33) (2018) 17132–17138, https://doi.org/10.1039/C8RA03075H.
- [79] H. Guo, et al., A novel Sm<sup>3+</sup> singly doped LiCa<sub>3</sub>ZnV<sub>3</sub>O<sub>12</sub> phosphor: a potential luminescent material for multifunctional applications, RSC Adv. 8 (58) (2018) 33403–33413, https://doi.org/10.1039/c8ra07329e.
- [80] J. Li, et al., The synergism between self-activated and impurity-related emissions of LiCa<sub>3</sub>ZnV<sub>3</sub>O<sub>12</sub>: lattice distortion, energy transfer and temperature sensing effect, RSC Adv. 12 (55) (2022) 36063–36071, https://doi.org/10.1039/d2ra06647e.
- [81] G.N. Warutkar, et al.,  $Nd^{3+}$  emission in the garnet structure of  $LiCa_3ZnV_3O_{12}$  phosphor, Radiat. Eff. Defects Solids 178 (11–12) (2023) 1479–1489, https://doi.org/10.1080/10420150.2023.2258435.
- [82] X. Zhou, et al., Eu<sup>3+</sup> activated LiSrVO<sub>4</sub> phosphors: emission color tuning and potential application in temperature sensing, Dyes Pigments 151 (2018) 219–226, https://doi.org/10.1016/j.dyepig.2017.12.059.
- [83] Y.-J. Hsiao, et al., Optical characteristics of LiZnVO<sub>4</sub> green phosphor at low temperature preparation, Mater. Lett. 70 (2012) 163–166, https://doi.org/10.1016/j.matlet.2011.11.076.
- [84] B.K. Grandhe, et al., Spectral characterization of novel LiZnVO<sub>4</sub> phosphor, Opt. Commun. 285 (6) (2012) 1194–1198, https://doi.org/10.1016/j.optcom.2011.10. 013
- [85] S. Khursheed, V. Kumar, J. Sharma, Effect of synthesis methods on structural, optical and spectral properties of bluish-green LiZnVO<sub>4</sub> phosphor, Mater. Focus 5 (2016) 1-4, https://doi.org/10.1002/chem.201402081.
- [86] F. Kang, et al., Abnormal anti-quenching and controllable multi-transitions of Bi<sup>3+</sup> luminescence by temperature in a yellow-emitting LuVO<sub>4</sub>:bi<sup>3+</sup> phosphor for UV-converted white LEDs, Chem. A Eur. J. 20 (36) (2014) 11522–11530, https://doi.org/10.1002/chem.201402081.
- [87] L. Zeng, et al., Fabrication of Bi<sup>3+</sup>/Ln<sup>3+</sup>:LuVO<sub>4</sub> (Ln = Eu, Sm, Dy, Ho) nanophosphors and its color-tunable optical performance, J. Lumin. 194 (2018) 667–674, https://doi.org/10.1016/j.jlumin.2017.09.033.
- [88] Y. Fujimoto, et al., Comparative study of optical and scintillation properties of YVO<sub>4</sub>, (Lu<sub>0.5</sub>Y<sub>0.5</sub>)VO<sub>4</sub>, and LuVO<sub>4</sub> single crystals, Nucl. Instrum. Methods Phys. Res., Sect. A, Accel. Spectrom. Detect. Assoc. Equip. 365 (1) (2011) 53–56, https://doi.org/10.1016/j.nima.2011.01.044.
- [89] H.W. Li, et al., Energy transfer mechanism and color-tunable luminescence properties of  ${\rm Eu}^{3+}$ -doped  ${\rm BaMg_2V_2O_8}$  vanadate phosphors, Chem. Phys. Lett. 662 (2016) 86–90, https://doi.org/10.1016/j.cplett.2016.09.032.
- [90] N. Sharma, P.P. Sahay, Structural, photoluminescence, and photocatalytic performances of Ce<sup>3+</sup>-activated orthovanadate oxides M<sub>3</sub>(VO<sub>4</sub>)<sub>2</sub> (M = Mg or Zn) synthesized by solution combustion route, Luminescence 39 (2) (2024) 4627, https://doi.org/10.1002/bio.4627.
- [91] D. Song, C. Guo, T. Li, Luminescence of the self-activated vanadate phosphors  $Na_2LnMg_2V_3O_{12}$  (Ln = Y, Gd), Ceram. Int. 41 (5) (2015) 6518–6524, https://doi.org/10.1016/j.ceramint.2015.01.094.

- [92] Y. Li, et al., A new self-activated vanadate phosphor of  $Na_2YMg_2(VO_4)_3$  and luminescence properties in  $Eu^{3+}$ -doped  $Na_2YMg_2(VO_4)_3$ , J. Lumin. 168 (2015) 124–129, https://doi.org/10.1016/j.jlumin.2015.08.002.
- [93] Y. Du, et al., Tunable luminescence in Eu $^{3+}$ /Sm $^{3+}$ -doped Na $_2$ YMg $_2$ V $_3$ O $_{12}$  for WLEDs and optical thermometry, Spectrochim. Acta, Part A, Mol. Biomol. Spectrosc. 330 (2025) 125759, https://doi.org/10.1016/j.saa.2025.125759.
- [94] W. Zhang, et al., Synthesis and photoluminescence properties of  $Eu^{3+}$ -doped  $Na_2YMg_2V_3O_{12}$ : a novel red-emitting phosphor for white-light-emitting diodes, Res. Sq. (2021), https://doi.org/10.21203/rs.3.rs-736843/v1.
- [95] Z. Li, Y. Li, A. Xia, Synthesis and luminescent properties of Eu<sup>3+</sup>-doped Na<sub>2</sub>YMg<sub>2</sub>(VO<sub>4</sub>)<sub>3</sub> phosphors, Chin. J. Lumin. 38 (3) (2017) 296–302, https://doi.org/10.3788/fgxb20173803.0296.
- [96] A.A. Setlur, et al., Spectroscopic evaluation of a white light phosphor for UV-LEDs-Ca<sub>2</sub>NaMg<sub>2</sub>V<sub>3</sub>O<sub>12</sub>:Eu<sup>3+</sup>, J. Electrochem. Soc. 152 (12) (2005) 205, https://doi.org/ 10.1149/1.2077328.
- [97] H. Zhou, et al., Ratiometric and colorimetric fluorescence temperature sensing properties of trivalent europium or samarium doped self-activated vanadate dualemitting phosphors, J. Lumin. 217 (2022) 116758, https://doi.org/10.1016/j. ilumin.2019.116758.
- [98] G. Warutkar, et al., Luminescence in NaCa $_2$ Mg $_2$ V $_3$ O $_{12}$  garnet, AIP Conf. Proc. 2974 (1) (2024) 020004, https://doi.org/10.1063/5.0181732.
- [99] D. Pasinski, J. Sokolnicki, Nitridated Ca<sub>2</sub>NaMg<sub>2</sub>V<sub>3</sub>O<sub>12</sub>:Eu<sup>3+</sup> vanadate garnet phosphor-in-glass, Materials 13 (2020) 2996, https://doi.org/10.3390/ ma13132996.
- [100] X. Chen, et al., Rare-earth free self-activated and rare-earth activated  $Ca_2NaZn_2V_3O_{12} \ \ vanadate \ phosphors \ and \ their \ color-tunable \ luminescence properties, \ J. Phys. Chem. Solids \ 74 \ (10) \ (2013) \ 1439–1443, \ https://doi.org/10.1016/j.jpcs.2013.05.002.$
- [101] L. Mi, et al., Modified optical properties via induced cation disorder in self-activated NaMg $_2$ V $_3$ O $_{10}$ , Dalton Trans. 47 (12) (2018) 4368–4376, https://doi.org/10.1039/C7DT04664B.
- [102] X. Nie, et al., Photoluminescence enhancement of self-activated vanadate NaMg<sub>4</sub>(VO<sub>4</sub>)<sub>3</sub> by cation substitutions, Mater. Lett. 185 (2016) 588–592, https://doi.org/10.1016/j.matlet.2016.07.016.
- [103] P. Dang, et al., Highly efficient cyan-green emission in self-activated Rb<sub>3</sub>RV<sub>2</sub>O<sub>8</sub> (R = Y, Lu) vanadate phosphors for full-spectrum white light-emitting diodes (LEDs), Inorg. Chem. 59 (9) (2020) 6026–6038, https://doi.org/10.1021/acs.inorgchem.0c00015
- [104] N. El Jouhari, et al., Luminescence of the Vanadate Group in phosphovanadates with general formula RbCaLa(PO<sub>4</sub>) $_{2-x}$ (VO<sub>4</sub>) $_x$  (0 < x  $\leq$  2), Phys. Inorg. Chem. 24 (19) (1993) 297–305, https://doi.org/10.1002/chin.199319015.
- [105] T. Ishigaki, et al., Room-temperature solid state contact reaction synthesis of rare earth free RbVO<sub>3</sub> phosphor and their photoluminescence properties, ECS J. Solid State Sci. Technol. 7 (6) (2018) R88, https://doi.org/10.1149/2.0201806jss.
- [106] S.W. Kim, et al., Improvement of luminescence properties of rubidium vanadate,  $RbVO_3$ , phosphors by erbium doping in the crystal lattice, New J. Chem. 41 (12) (2017) 4788–4792, https://doi.org/10.1039/c6nj03823a.
- [107] X. Kang, et al., Uniform REVO<sub>4</sub>:Bi<sup>3+</sup> micro/nanocrystals via hydrothermal reaction, microstructure, and widely tunable broadband luminescence (RE = Sc, Lu, Y, Gd,  $Lu_{0.5}Sc_{0.5}$ ,  $Y_{0.5}Lu_{0.5}$ ,  $Gd_{0.5}Y_{0.5}$ ), Ceram. Int. 51 (2) (2025) 2324–2334, https://doi.org/10.1016/j.ceramint.2024.11.213.
- [108] F. Kang, et al., Red photoluminescence from Bi<sup>3+</sup> and the influence of the oxygen-vacancy perturbation in ScVO<sub>4</sub>: a combined experimental and theoretical study, J. Phys. Chem. C 118 (14) (2014) 7515–7522, https://doi.org/10.1021/jp4081965.
- [109] F. Kang, et al., Luminescence in external dopant-free scandium-phosphorus vanadate solid solution: a spectroscopic and theoretical investigation, Mater. Adv. 1 (7) (2020) 2467–2482, https://doi.org/10.1039/D0MA00438C.
- [110] J. Zhou, et al., Luminescence study of a self-activated and rare earth activated  $Sr_3La(VO_4)_3$  phosphor potentially applicable in W-LEDs, J. Mater. Chem. C 3 (13) (2015) 3023–3028, https://doi.org/10.1039/c4tc02783c.
- [111] N.S. Sawala, N.S. Bajaj, S.K. Omanwar, Near-infrared quantum cutting in Yb<sup>3+</sup> ion doped strontium vanadate, Infrared Phys. Technol. 76 (2016) 271–275, https://doi.org/10.1016/j.infrared.2016.03.007.
- [112] P. Woźny, et al., Structure-dependent luminescence of Eu<sup>3+</sup>-doped strontium vanadates synthesized with different V ratios application in WLEDs and ultra-sensitive optical thermometry, J. Mater. Chem. C 11 (14) (2023) 4792–4807, https://doi.org/10.1039/d2tc05341a.
- [113] L. Mi, et al., Improvement of self-activated luminescence from introduced cation disorder in  $Sr_6V_2O_{11}$ , J. Am. Ceram. Soc. 101 (7) (2018) 2987–2995, https://doi.org/10.1111/jace.15448.
- [114] J. Su, et al., Tunable luminescence and energy transfer properties in  $YVO_4$ :Bi<sup>3+</sup>, Eu<sup>3+</sup> phosphors, J. Mater. Sci. 52 (2017) 782–792, https://doi.org/10.1007/s10853-016-0375-9.
- [115] F. Wang, et al., Defect control and optical performance of yttrium orthovanadate nanocrystals via a facile pH-sensitive synthesis, J. Alloys Compd. 968 (2023) 172259, https://doi.org/10.1016/j.jallcom.2023.172259.
- [116] R.V. Perrella, et al., The influence of defects on the luminescence of trivalent terbium in nanocrystalline yttrium orthovanadate, Nano Lett. 22 (9) (2022) 3569–3575, https://doi.org/10.1021/acs.nanolett.1c04937.

- [117] E. Cavalli, et al., Tunable luminescence of  $\mathrm{Bi^{3+}}$ -doped  $\mathrm{YP_xV_{1-x}O_4}$  ( $0 \le x \le 1$ ), J. Phys. Condens. Matter 26 (38) (2014) 385503, https://doi.org/10.1088/0953-8984/26/38/385503.
- [118] W. Xie, et al., Toward temperature-dependent Bi<sup>3+</sup>-related tunable emission in the YVO<sub>4</sub>:Bi<sup>3+</sup> phosphor, J. Am. Ceram. Soc. 102 (6) (2019) 3488–3497, https://doi.org/10.1111/jace.16188
- [119] M.A. Aia, Structure and luminescence of the phosphate-Vanadates of yttrium, gadolinium, lutetium, and lanthanum, J. Electrochem. Soc. 114 (4) (1967) 367, https://doi.org/10.1149/1.2426598.
- [120] S.-P. Kuang, et al., A new self-activated yellow-emitting phosphor Zn<sub>2</sub>V<sub>2</sub>O<sub>7</sub> for white LED, Optik 124 (22) (2013) 5517–5519, https://doi.org/10.1016/j.ijleo. 2013 03 172
- [121] A.V. Ishchenko, et al., Influence of grain size on luminescence properties of microand nanopowder Zn<sub>2</sub>V<sub>2</sub>O<sub>7</sub> vanadate, Radiat. Meas. 90 (2016) 33–37, https://doi. org/10.1016/j.radmeas.2016.01.030.
- [122] T. Li, et al., Fabrication and characterization of Zn<sub>3</sub>V<sub>2</sub>O<sub>8</sub> phosphor by sol-gel process, J. Sol-Gel Sci. Technol. 66 (2013) 225–230, https://doi.org/10.1007/s10971-013-2997-6
- [123] T. Qian, et al., Structure and luminescence properties of Zn<sub>3</sub>V<sub>2</sub>O<sub>8</sub> yellow phosphor for white light emitting diodes, Chem. Phys. Lett. 715 (2019) 34–39, https://doi. org/10.1016/j.cplett.2018.11.022.
- [124] V. Chauhan, et al., Greenish-yellow emission from rare-earth free Li<sup>+</sup> doped zinc vanadate phosphor, Results Phys. 39 (2022) 105689, https://doi.org/10.1016/j. rinp.2022.105689.
- [125] J. Luo, R. Chen, X. Zhang, Effect of solvent on the luminescence properties of Zn<sub>3</sub>V<sub>2</sub>O<sub>8</sub> and the first principle calculation of α-Zn<sub>3</sub>V<sub>2</sub>O<sub>8</sub>, IOP Conf. Ser., Mater. Sci. Eng. 274 (2017) 012145, https://doi.org/10.1088/1757-899X/274/1/ 012145
- [126] H.N. Luitel, et al., Rare earth free  $\rm Zn_3V_2O_8$  phosphor with controlled microstructure and its photocatalytic activity, Int. J. Photoenergy 13 (2013) 410613, https://doi.org/10.1155/2013/410613.
- [127] J. Luo, et al., The effect in the crystal phase and luminescence property of Zn<sub>3</sub>V<sub>2</sub>O<sub>8</sub> with calcination temperature, Int. Conf. Adv. Mater. Inf. Technol. Process. (2016), https://doi.org/10.2991/amitp-16.2016.29.
- [128] J. Luo, et al., The effect in the production and luminescence property of Zn<sub>3</sub>V<sub>2</sub>O<sub>8</sub> with Eu-doping, Int. Conf. Adv. Mater. Inf. Technol. Process. (2016), https://doi.org/10.2991/amitp-16.2016.64.
- [129] T. Li, et al., Sintering condition and optical properties of  $Zn_3V_2O_8$  phosphor, Adv. Mater. Phys. Chem. 2 (2012) 173–177, https://doi.org/10.4236/ampc.2012.
- $[130] \ B.V.\ Shul'gin,\ et\ al.,\ Excitation\ spectra\ of\ vanadates,\ J.\ Appl.\ Spectrosc.\ 23\ (1975)\\ 1126-1128,\ https://doi.org/10.1007/BF00611763.$
- [131] H. Ronde, J.G. Snijder, The position of the VO<sub>4</sub><sup>3-</sup> charge-transfer transition as a function of the V O distance, Chem. Phys. Lett. 50 (2) (1977) 282–283, https://doi.org/10.1016/0009-2614(77)80182-6.
- [132] G. Blasse, Some considerations and experiments on concentration quenching of characteristic broad-band fluorescence, Philips Res. Rep. 23 (1968) 344–361.
- [133] C. Hsu, R.C. Powell, Energy transfer in europium doped yttrium vanadate crystals, J. Lumin. 10 (5) (1975) 273–293, https://doi.org/10.1016/0022-2313(75)90051-4
- [134] R.C. Powell, G. Blasse, Energy Transfer in Concentrated Systems, Luminescence and Energy Transfer. Structure and Bonding., vol. 42, Springer, Berlin, Heidelberg, 1980, pp. 43–96.

- [135] J. Zhang, et al., Bimolecular self-trapped exciton formation in bismuth vanadate, J. Phys. Chem. Lett. 13 (42) (2022) 9815–9821, https://doi.org/10.1021/acs.jpclett. 2c02596.
- [136] Z. Feng, et al., Self-activated and bismuth-related photoluminescence in rareearth vanadate, niobate, and tantalate series—a first-principles study, Inorg. Chem. 60 (21) (2021) 16614–16625, https://doi.org/10.1021/acs.inorgchem.1c02508.
- [137] H.A. Jahn, E. Teller, Stability of polyatomic molecules in degenerate electronic states - I—orbital degeneracy, Proc. R. Soc. Lond. A 161 (905) (1937) 220–235, https://doi.org/10.1098/rspa.1937.0142.
- [138] W. Barendswaard, R.T. Weber, J.H. van der Waals, An EPR study of the luminescent triplet state of  ${\rm VO_4}^{3-}$  in  ${\rm YVO_4}$  and  ${\rm YP_{0.96}V_{0.04}O_4}$  single crystals at 1.2 K, J. Chem. Phys. 87 (7) (1987) 3731–3738, https://doi.org/10.1063/1.452927.
- [139] W. Barendswaard, J. van Tol, J.H. van der Waals, The metastable triplet states of K<sub>2</sub>Cr<sub>2</sub>O<sub>7</sub> and YVO<sub>4</sub> at 1.2 K: zero-field splitting and lifetimes of the spin components, Chem. Phys. Lett. 121 (4–5) (1985) 361–366, https://doi.org/10.1016/ 0009-2614(85)87194-3
- [140] W. Barendswaard, et al., The luminescent triplet state of the  $Ba_3(VO_4)_2$  crystal, Mol. Phys. 67 (3) (1989) 651–664, https://doi.org/10.1080/00268978900101341.
- [141] C.J.M. Coremans, E.J.J. Groenen, J.H. van der Waals, The metastable triplet state of CrO<sub>4</sub><sup>2-</sup> in a calcium sulphate host: electron-spin-echo experiments, J. Chem. Phys. 93 (5) (1990) 3101–3110, https://doi.org/10.1063/1.458844.
- [142] Y. Matsushima, et al., The determining factor of the luminescence energies of vanadate phosphors, J. Ceram. Soc. Jpn. 127 (9) (2019) 627–635, https://doi.org/10. 2109/jcersj2.19113.
- [143] S.L. Berdnikov, Ya.M. Zelikin, Luminescence, excitation, and absorption spectra of alkali metal metavanadate single crystals, Opt. Spektrosk. 53 (3) (1983) 464–470.
- [144] G. Blasse, Luminescence of inorganic solids, Rev. Inorg. Chem. 5 (4) (1983) 319–381.
- [145] N.F. Mott, A.M. Stoneham, The lifetime of electrons, holes and excitons before self-trapping, J. Phys. C, Solid State Phys. 10 (1977) 3391–3398, https://doi.org/10.1088/0022-3719/10/17/022.
- [146] S. Yuan, et al., Ab initio insight into the formation of small polarons: a study across four metal peroxides, Phys. Rev. B 100 (20) (2019) 205201, https://doi.org/10. 1103/PhysRevB.100.205201.
- [147] G. Blasse, Thermal quenching of characteristic luminescence. II, J. Solid State Chem. 9 (2) (1974) 147–151, https://doi.org/10.1016/0022-4596(74)90066-8.
- [148] G. Blasse, A. Bril, Photoluminescent efficiency of phosphors with electronic transitions in localized centers, J. Electrochem. Soc. 115 (10) (1968) 1067–1075, https:// doi.org/10.1149/1.2410880.
- [149] G. Blasse, A. Bril, The influence of crystal structure on the fluorescence of oxidic niobates and related compounds, Z. Phys. Chem. 57 (3–6) (1968) 187–202, https://doi.org/10.1524/zpch.1968.57.3\_6.187.
- [150] D.L. Dexter, C.C. Klick, G.A. Russell, Criterion for the occurrence of luminescence, Phys. Rev. 100 (2) (1955) 603–605, https://doi.org/10.1103/PhysRev.100.603.
- [151] G. Blasse, Materials science of the luminescence of inorganic solids, in: B. Di Bartolo, V. Godberg, D. Pacheco (Eds.), Luminescence of Inorganic Solids, Springer, Boston, MA, 1978, pp. 457–494.
- [152] F.C. Hawthorne, C. Calvo, The crystal chemistry of the  $M^+VO_3$  ( $M^+=Li$ , Na, K, NH<sub>4</sub>, Tl, Rb, and Cs) pyroxenes, J. Solid State Chem. 22 (2) (1977) 157–170, https://doi.org/10.1016/0022-4596(77)90033-0.